Supporting Information For

Reduction of Benzonitriles via Osmium-Azavinylidene Intermediates Bearing Nucleophilic and Electrophilic Centers

Juan C. Babón,[†] Miguel A. Esteruelas,*[†] Israel Fernández,[‡] Ana M. López,[†] and Enrique Oñate[†]

[†]Departamento de Química Inorgánica, Instituto de Síntesis Química y Catálisis Homogénea (ISQCH), Centro de Innovación en Química Avanzada (ORFEO-CINQA), Universidad de Zaragoza-CSIC, 50009 Zaragoza, Spain.

[‡]Departamento de Química Orgánica I, Facultad de Ciencias Químicas, Centro de Innovación en Química Avanzada (ORFEO-CINQA), Universidad Complutense de Madrid, 28040 Madrid, Spain.

* Corresponding author's e-mail address: maester@unizar.es

Contents:

General information. All manipulations were performed with rigorous exclusion of air at an argon/vacuum manifold using standard Schlenk-tube or glovebox techniques. Solvents were dried by the usual procedures and distilled under argon prior to use or obtained oxygen- and water-free from an MBraun solvent purification apparatus. Pentane was stored over P_2O_5 in the glovebox. Toluene, THF, and benzene were stored over sodium in the glovebox. NMR spectra were recorded on a Bruker ARX 300, Bruker Avance 300 MHz, or a Bruker Avance 400 MHz instruments. Chemical shifts (expressed in parts per million) are referenced to residual solvent peaks (^{1}H, ^{13}C{^{1}H}), external H_3PO_4 (^{31}P{^{1}H}). Coupling constants, *J*, and *N* ($N = {}^3J_{H\text{-}P} + {}^5J_{H\text{-}P'}$ for ^{1}H or ${}^1J_{C\text{-}P} + {}^3J_{C\text{-}P'}$ for ^{13}C) are given in Hertz. C and H analyses were carried out in a Perkin-Elmer 2400 CHNS/O analyzer. Attenuated total reflection infrared spectra (ATR-IR) of solid samples were run on a Perkin-Elmer Spectrum 100 FT-IR spectrometer.

Structural Analysis of Complexes 2, 3, and 5. X-ray data were collected on a Bruker Smart APEX CCD diffractometer equipped with a normal focus, and 2.4 kW sealed tube source (Mo radiation, $\lambda = 0.71073$ Å). Data were collected over the complete sphere covering 0.3° in ω. Data were corrected for absorption by using a multiscan method applied with the SADABS program.[1] The structures were solved by Patterson or direct methods and refined by full-matrix least squares on F^2 with SHELXL2016,[2] including isotropic and subsequently anisotropic displacement parameters. The hydrogen atoms were observed in the least-squares Fourier maps or calculated, and were refined freely or using a restricted riding model. The hydrides were observed in the last difference Fourier maps, but refined with restrained Os-H distance ($d_{Os\text{-}H} = 1.59$ Å).

Crystal data for **2**: $C_{27}H_{55}NOsP_2$, M_W 645.86, dark orange, irregular block (0.135 x 0.133 x 0.114 mm^3), tetragonal, space group P41212, *a*: 11.1678(6) Å, *b*: 11.1678(6) Å, *c*: 48.728(3) Å, $V = 6077.3(7)$ Å^3, $Z = 8$, $Z' = 1$, D_{calc}: 1.412 g cm^{-3}, F(000): 2640, $T = 100(2)$ K, μ 4.316 mm^{-1}. 60768 measured reflections (2θ: 3-57°, ω scans 0.3°), 7567 unique ($R_{int} = 0.0719$); min./max. transm. Factors 0.603/0.746. Final agreement factors were $R^1 = 0.0352$ (6138 observed reflections, $I > 2\sigma(I)$) and $wR^2 = 0.0735$; data/restraints/parameters 7567/4/293; GoF = 1.013. Largest peak and hole 1.533 (close to osmium atoms) and -0.764 e/ Å^3.

Crystal data for **3**: $C_{25}H_{51}NOsP_2$, M_W 617.80, orange, irregular block (0.153 x 0.121 x 0.105 mm^3), monoclinic, space group $P2_1/n$, *a*: 7.8436(7) Å, *b*: 14.6943(13) Å, *c*:

24.350(2) Å, β: 90.2020(10)°, V = 2806.5(4) Å^3, Z = 4, Z' = 1, D_{calc}: 1.462 g cm^{-3}, F(000): 1256, T = 100(2) K, μ 4.669 mm^{-1}. 48869 measured reflections (2θ: 3-57°, ω scans 0.3°), 6911 unique (R_{int} = 0.0564); min./max. transm. Factors 0.598/0.862. Final agreement factors were R^1 = 0.0301 (5864 observed reflections, I > 2σ(I)) and wR^2 = 0.0742; data/restraints/parameters 6911/3/286; GoF = 1.031. Largest peak and hole 2.153 (close to osmium atoms) and -2.280 e/ Å^3.

Crystal data for **5**: $C_{25}H_{51}NOsP_2$, M_w 617.80, red, irregular block (0.160 x 0.128 x 0.113 mm^3), monoclinic, space group $P2_1/n$, a: 12.9546(7) Å, b: 10.2134(5) Å, c: 21.2423(11) Å, β: 105.6890(10)°, V = 2705.9(2) Å^3, Z = 4, Z' = 1, D_{calc}: 1.517 g cm^{-3}, F(000): 1256, T = 100(2) K, μ 4.843 mm^{-1}. 46548 measured reflections (2θ: 3-57°, ω scans 0.3°), 6656 unique (R_{int} = 0.0369); min./max. transm. Factors 0.678/0.862. Final agreement factors were R^1 = 0.0349 (6026 observed reflections, I > 2σ(I)) and wR^2 = 0.0681; data/restraints/parameters 6656/3/289; GoF = 1.055. Largest peak and hole 5.854 (close to osmium atoms) and -2.900 e/ Å^3.

Computational Details

Bonding analysis: Geometry optimizations of complex **3**, $OsCl_3(=N=CHPh)(P^iPr_3)_2$ and $OsHCl_2(=N=CHPh)(P^iPr_3)_2$ were performed without symmetry constraints using the Gaussian09[3] suite of programs at the BP86[4]/def2-SVP[5] level of theory using the D3 dispersion correction suggested by Grimme et al.[6] This level is denoted BP86-D3/def2-SVP. These species were also characterized by frequency calculations, and have positive definite Hessian matrices thus confirming that the computed structures are minima on the potential energy surface.

The interaction between the transition metal fragment and azavinylidene ligand in these complexes has been investigated with the EDA-NOCV method,[7] which combines the energy decomposition analysis (EDA)[8] with the natural orbitals for chemical valence (NOCV)[9] methods. Within this approach, the interaction energy can be decomposed into the following physically meaningful terms:

$$\Delta E_{int} = \Delta E_{elstat} + \Delta E_{Pauli} + \Delta E_{orb} + \Delta E_{disp}$$

The term ΔE_{elstat} corresponds to the classical electrostatic interaction between the unperturbed charge distributions of the deformed reactants and is usually attractive. The Pauli repulsion ΔE_{Pauli} comprises the destabilizing interactions between occupied

orbitals and is responsible for any steric repulsion. The orbital interaction ΔE_{orb} accounts for charge transfer (interaction between occupied orbitals on one moiety with unoccupied orbitals on the other, including HOMO–LUMO interactions) and polarization (empty-occupied orbital mixing on one fragment due to the presence of another fragment). Finally, the ΔE_{disp} term takes into account the interactions which are due to dispersion forces.

The EDA-NOCV method makes it possible to further partition the total orbital interactions into pairwise contributions of the orbital interactions. Details of the method can be found in the literature.[10]

The EDA-NOCV calculations were carried out using the BP86-D3/def2-TZVPP optimized geometry with the program package ADF 2017.01[11] using the same functional (BP86-D3) in conjunction with a triple-ζ-quality basis set using uncontracted Slater-type orbitals (STOs) augmented by two sets of polarization function with a frozen-core approximation for the core electrons.[12] An auxiliary set of s, p, d, f, and g STOs were used to fit the molecular densities and to represent the Coulomb and exchange potentials accurately in each SCF cycle.[13] Scalar relativistic effects were incorporated by applying the zeroth-order regular approximation (ZORA).[14] This level of theory is denoted BP86-D3/TZ2P//BP86-D3/def2-SVP.

Table S1. Results of the EDA-NOCV calculations of model complexes $OsH_3(=N=CHPh)(PMe_3)_2$ and $OsCl_3(=N=CHPh)(PMe_3)_2$ at the BP86-D3/TZ2P//RI-BP86-D3/def2-TZVPP level. Energy values are given in kcal mol^{-1}.[a]

	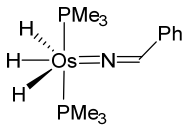			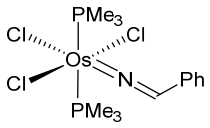		
	Donor-acceptor	**Electron-sharing/Donor-acceptor**	**Electron-sharing**	**Donor-acceptor**	**Electron-sharing/Donor-acceptor**	**Electron-sharing/**
Fragments	$[Os]^+$	$[Os]^\bullet$ (d)	$[Os]^{\bullet\bullet\bullet}$ (q)	$[Os]^+$	$[Os]^\bullet$ (d)	$[Os]^{\bullet\bullet\bullet}$ (q)
	$[N{=}CHPh]^-$	$[N{=}CHPh]^\bullet$ (d)	$[N{=}CHPh]^{\bullet\bullet\bullet}$ (q)	$[N{=}CHPh]^-$	$[N{=}CHPh]^\bullet$ (d)	$[N{=}CHPh]^{\bullet\bullet\bullet}$ (q)
ΔE_{int}	-206.5	-110.4	-275.7	-253.0	98.4	-238.8
ΔE_{Pauli}	232.0	201.7	323.4	341.6	280.2	384.3
ΔE_{elstat}	-280.9	-143.3	-199.0	-341.6	-186.8	-230.9
ΔE_{orb}	-147.1	-158.3	-389.7	-242.2	-181.0	-381.4
ΔE_{disp}	-10.4	-10.4	-10.4	-10.7	-10.7	-10.7
$\Delta E_{orb}(\rho 1)$	-51.4	-84.1	-271.0	-99.8	-67.0	-252.1
$\Delta E_{orb}(\rho 2)$	-26.4	-26.5	-72.7	-33.9	-35.1	-63.9
$\Delta E_{orb}(\rho 3)$	-44.4	-34.6	-25.5	-79.9	-63.8	-41.0
ΔE_{orb}(rest)	-24.9	-13.1	-20.5	-28.6	-15.1	-24.4

[a]Energy values are given in kcal mol^{-1}.

Total energies (in a. u., non corrected zero-point vibrational energies included) of **3**, $OsCl_3(=N=CHPh)(P^iPr_3)_2$ and $OsHCl_2(=N=CHPh)(P^iPr_3)_2$ (BP86-D3/def2-SVP level).

3: E= -1810.271143

$OsCl_3(=N=CHPh)(P^iPr_3)_2$: E= -3188.929810

$OsHCl_2(=N=CHPh)(P^iPr_3)_2$: E= -2729.388264

Complete energy values of complexes included in the mechanistic studies (B3LYP-D3/SDD/6-31G** level)**:**

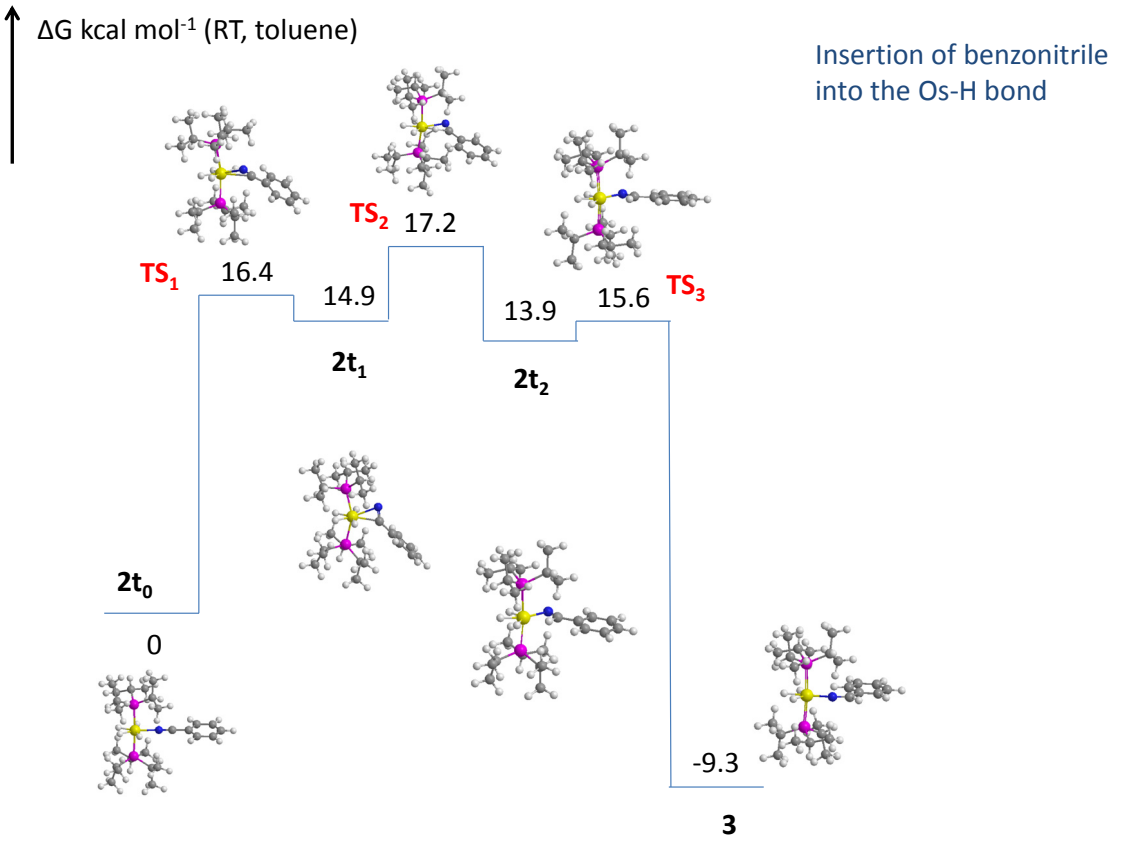

Figure S1. Computed energy profile for the nitrile insertion into one of the Os-H bonds.

$2t_0$

Zero-point correction=	0.708757 (Hartree/Particle)
Thermal correction to Energy=	0.748692
Thermal correction to Enthalpy=	0.749637
Thermal correction to Gibbs Free Energy=	0.636520
Sum of electronic and zero-point Energies=	-1811.124874
Sum of electronic and thermal Energies=	-1811.084939
Sum of electronic and thermal Enthalpies=	-1811.083994
Sum of electronic and thermal Free Energies=	-1811.197111

TS_1

Zero-point correction=	0.707311 (Hartree/Particle)
Thermal correction to Energy=	0.747019
Thermal correction to Enthalpy=	0.747963
Thermal correction to Gibbs Free Energy=	0.637395
Sum of electronic and zero-point Energies=	-1811.101098
Sum of electronic and thermal Energies=	-1811.061390
Sum of electronic and thermal Enthalpies=	-1811.060446
Sum of electronic and thermal Free Energies=	-1811.171015

$2t_1$

Zero-point correction= 0.710933 (Hartree/Particle)
Thermal correction to Energy= 0.750151
Thermal correction to Enthalpy= 0.751095
Thermal correction to Gibbs Free Energy= 0.642157
Sum of electronic and zero-point Energies= -1811.104609
Sum of electronic and thermal Energies= -1811.065391
Sum of electronic and thermal Enthalpies= -1811.064447
Sum of electronic and thermal Free Energies= -1811.173385

TS_2

Zero-point correction= 0.708219 (Hartree/Particle)
Thermal correction to Energy= 0.747368
Thermal correction to Enthalpy= 0.748312
Thermal correction to Gibbs Free Energy= 0.639913
Sum of electronic and zero-point Energies= -1811.101453
Sum of electronic and thermal Energies= -1811.062304
Sum of electronic and thermal Enthalpies= -1811.061360
Sum of electronic and thermal Free Energies= -1811.169759

$2t_2$

Zero-point correction= 0.710479 (Hartree/Particle)
Thermal correction to Energy= 0.750047
Thermal correction to Enthalpy= 0.750991
Thermal correction to Gibbs Free Energy= 0.639932
Sum of electronic and zero-point Energies= -1811.104478
Sum of electronic and thermal Energies= -1811.064909
Sum of electronic and thermal Enthalpies= -1811.063965
Sum of electronic and thermal Free Energies= -1811.175024

TS_3

Zero-point correction= 0.710525 (Hartree/Particle)
Thermal correction to Energy= 0.749572
Thermal correction to Enthalpy= 0.750516
Thermal correction to Gibbs Free Energy= 0.640665
Sum of electronic and zero-point Energies= -1811.102449
Sum of electronic and thermal Energies= -1811.063402
Sum of electronic and thermal Enthalpies= -1811.062458
Sum of electronic and thermal Free Energies= -1811.172309

3

Zero-point correction= 0.712767 (Hartree/Particle)
Thermal correction to Energy= 0.752245
Thermal correction to Enthalpy= 0.753189
Thermal correction to Gibbs Free Energy= 0.642490
Sum of electronic and zero-point Energies= -1811.141716
Sum of electronic and thermal Energies= -1811.102239

Sum of electronic and thermal Enthalpies= -1811.101294
Sum of electronic and thermal Free Energies= -1811.211994

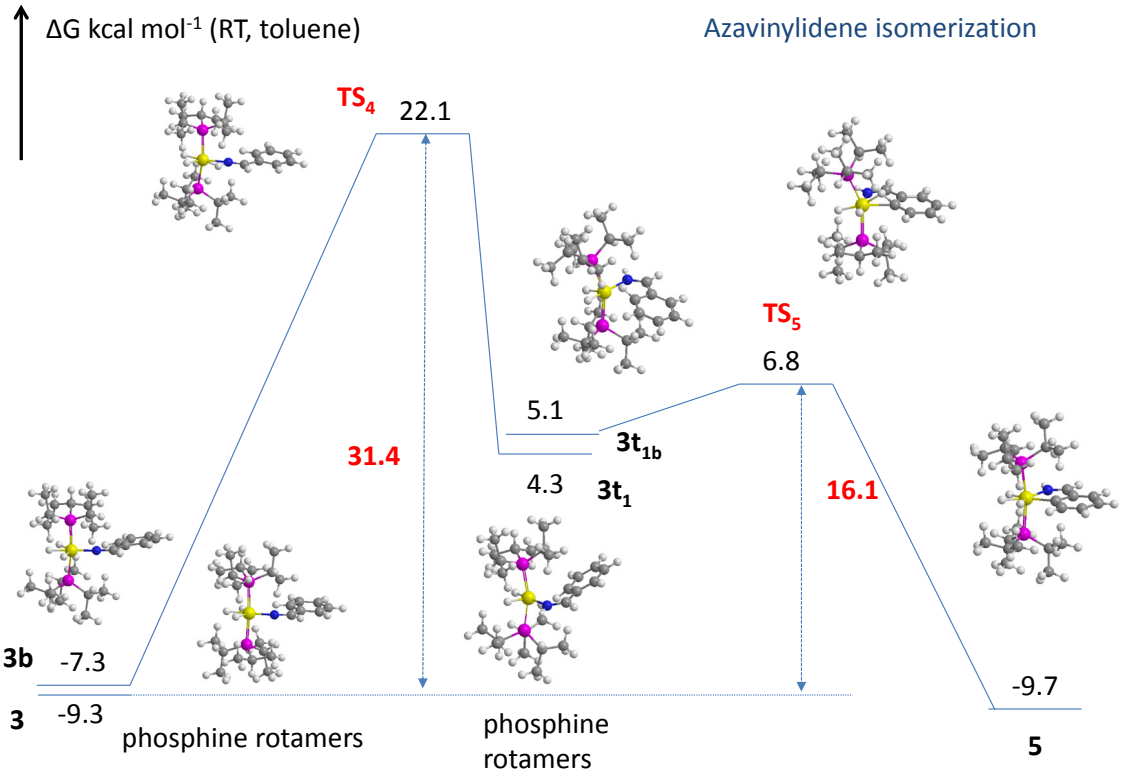

Figure S2. Computed energy profile for the isomerization of **3** into **5**.

3b

Zero-point correction= 0.712790 (Hartree/Particle)
Thermal correction to Energy= 0.752240
Thermal correction to Enthalpy= 0.753185
Thermal correction to Gibbs Free Energy= 0.642839
Sum of electronic and zero-point Energies= -1811.138820
Sum of electronic and thermal Energies= -1811.099369
Sum of electronic and thermal Enthalpies= -1811.098424
Sum of electronic and thermal Free Energies= -1811.208771

TS_4

Zero-point correction= 0.711039 (Hartree/Particle)
Thermal correction to Energy= 0.750129
Thermal correction to Enthalpy= 0.751073
Thermal correction to Gibbs Free Energy= 0.641663
Sum of electronic and zero-point Energies= -1811.092550
Sum of electronic and thermal Energies= -1811.053460
Sum of electronic and thermal Enthalpies= -1811.052516
Sum of electronic and thermal Free Energies= -1811.161926

$3t_1$

Zero-point correction= 0.719193 (Hartree/Particle)
Thermal correction to Energy= 0.758076
Thermal correction to Enthalpy= 0.759020
Thermal correction to Gibbs Free Energy= 0.650204
Sum of electronic and zero-point Energies= -1811.121210
Sum of electronic and thermal Energies= -1811.082327
Sum of electronic and thermal Enthalpies= -1811.081383
Sum of electronic and thermal Free Energies= -1811.190200

$3t_{1b}$

Zero-point correction= 0.716241 (Hartree/Particle)
Thermal correction to Energy= 0.754820
Thermal correction to Enthalpy= 0.755764
Thermal correction to Gibbs Free Energy= 0.648796
Sum of electronic and zero-point Energies= -1811.121510
Sum of electronic and thermal Energies= -1811.082932
Sum of electronic and thermal Enthalpies= -1811.081988
Sum of electronic and thermal Free Energies= -1811.188956

TS_5

Zero-point correction= 0.713430 (Hartree/Particle)
Thermal correction to Energy= 0.751490
Thermal correction to Enthalpy= 0.752434
Thermal correction to Gibbs Free Energy= 0.647358
Sum of electronic and zero-point Energies= -1811.120228
Sum of electronic and thermal Energies= -1811.082168
Sum of electronic and thermal Enthalpies= -1811.081224
Sum of electronic and thermal Free Energies= -1811.186300

5

Zero-point correction= 0.715015 (Hartree/Particle)
Thermal correction to Energy= 0.753321
Thermal correction to Enthalpy= 0.754265
Thermal correction to Gibbs Free Energy= 0.648985
Sum of electronic and zero-point Energies= -1811.146562
Sum of electronic and thermal Energies= -1811.108256
Sum of electronic and thermal Enthalpies= -1811.107312
Sum of electronic and thermal Free Energies= -1811.212591

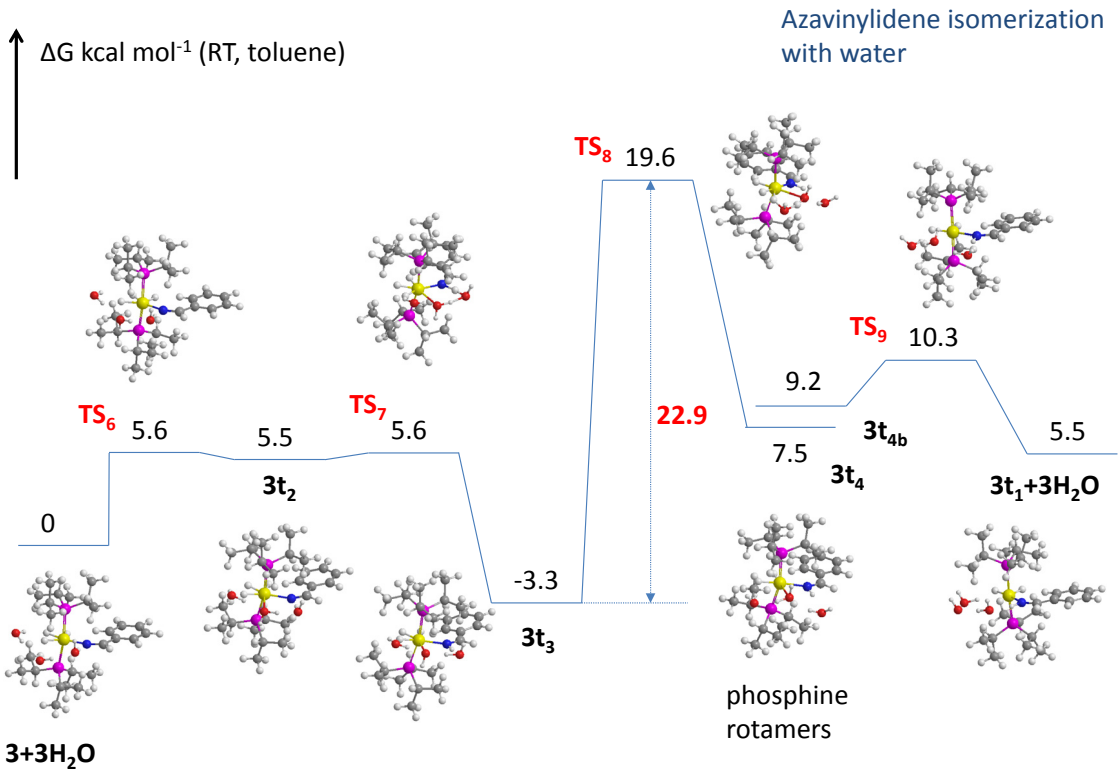

Figure S3. Computed energy profile for the water-assisted hydride migration.

3+3H_2O

Zero-point correction= 0.790162 (Hartree/Particle)
Thermal correction to Energy= 0.837547
Thermal correction to Enthalpy= 0.838491
Thermal correction to Gibbs Free Energy= 0.712954
Sum of electronic and zero-point Energies= -2040.399082
Sum of electronic and thermal Energies= -2040.351698
Sum of electronic and thermal Enthalpies= -2040.350754
Sum of electronic and thermal Free Energies= -2040.476290

TS_6

Zero-point correction= 0.789928 (Hartree/Particle)
Thermal correction to Energy= 0.836477
Thermal correction to Enthalpy= 0.837421
Thermal correction to Gibbs Free Energy= 0.712936
Sum of electronic and zero-point Energies= -2040.390839
Sum of electronic and thermal Energies= -2040.344289
Sum of electronic and thermal Enthalpies= -2040.343345
Sum of electronic and thermal Free Energies= -2040.467831

$3t_2$

Zero-point correction= 0.791069 (Hartree/Particle)
Thermal correction to Energy= 0.837283
Thermal correction to Enthalpy= 0.838227

Thermal correction to Gibbs Free Energy= 0.715459
Sum of electronic and zero-point Energies= -2040.391891
Sum of electronic and thermal Energies= -2040.345678
Sum of electronic and thermal Enthalpies= -2040.344733
Sum of electronic and thermal Free Energies= -2040.467501

TS_7

Zero-point correction= 0.787125 (Hartree/Particle)
Thermal correction to Energy= 0.832548
Thermal correction to Enthalpy= 0.833492
Thermal correction to Gibbs Free Energy= 0.711803
Sum of electronic and zero-point Energies= -2040.394265
Sum of electronic and thermal Energies= -2040.348843
Sum of electronic and thermal Enthalpies= -2040.347898
Sum of electronic and thermal Free Energies= -2040.469587

$3t_3$

Zero-point correction= 0.793835 (Hartree/Particle)
Thermal correction to Energy= 0.839596
Thermal correction to Enthalpy= 0.840541
Thermal correction to Gibbs Free Energy= 0.719613
Sum of electronic and zero-point Energies= -2040.407329
Sum of electronic and thermal Energies= -2040.361568
Sum of electronic and thermal Enthalpies= -2040.360624
Sum of electronic and thermal Free Energies= -2040.481551

TS_8

Zero-point correction= 0.787954 (Hartree/Particle)
Thermal correction to Energy= 0.833227
Thermal correction to Enthalpy= 0.834171
Thermal correction to Gibbs Free Energy= 0.713853
Sum of electronic and zero-point Energies= -2040.371007
Sum of electronic and thermal Energies= -2040.325734
Sum of electronic and thermal Enthalpies= -2040.324790
Sum of electronic and thermal Free Energies= -2040.445107

$3t_4$

Zero-point correction= 0.793516 (Hartree/Particle)
Thermal correction to Energy= 0.840323
Thermal correction to Enthalpy= 0.841267
Thermal correction to Gibbs Free Energy= 0.716192
Sum of electronic and zero-point Energies= -2040.387082
Sum of electronic and thermal Energies= -2040.340276
Sum of electronic and thermal Enthalpies= -2040.339331
Sum of electronic and thermal Free Energies= -2040.464406

TS_9

Zero-point correction= 0.792959 (Hartree/Particle)
Thermal correction to Energy= 0.839130
Thermal correction to Enthalpy= 0.840074
Thermal correction to Gibbs Free Energy= 0.717721
Sum of electronic and zero-point Energies= -2040.384588
Sum of electronic and thermal Energies= -2040.338417
Sum of electronic and thermal Enthalpies= -2040.337473
Sum of electronic and thermal Free Energies= -2040.459827

3t$_1$+3H$_2$O

Zero-point correction= 0.791067 (Hartree/Particle)
Thermal correction to Energy= 0.837281
Thermal correction to Enthalpy= 0.838225
Thermal correction to Gibbs Free Energy= 0.715458
Sum of electronic and zero-point Energies= -2040.391892
Sum of electronic and thermal Energies= -2040.345678
Sum of electronic and thermal Enthalpies= -2040.344734
Sum of electronic and thermal Free Energies= -2040.467502

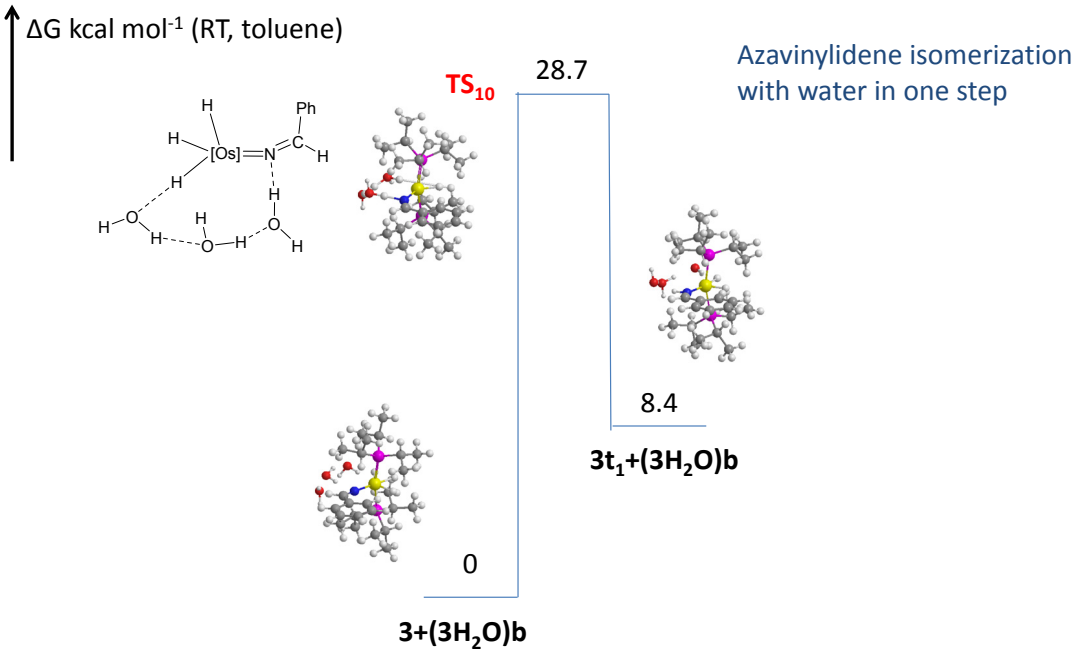

Figure S4. Computed energy profile for the water-assisted hydride migration in one step.

3+(3H$_2$O)b

Zero-point correction= 0.790377 (Hartree/Particle)
Thermal correction to Energy= 0.837484
Thermal correction to Enthalpy= 0.838429
Thermal correction to Gibbs Free Energy= 0.712822
Sum of electronic and zero-point Energies= -2040.402202
Sum of electronic and thermal Energies= -2040.355095
Sum of electronic and thermal Enthalpies= -2040.354151

Sum of electronic and thermal Free Energies= -2040.479757

TS10

Zero-point correction= 0.782934 (Hartree/Particle)
Thermal correction to Energy= 0.827612
Thermal correction to Enthalpy= 0.828556
Thermal correction to Gibbs Free Energy= 0.708908
Sum of electronic and zero-point Energies= -2040.359944
Sum of electronic and thermal Energies= -2040.315266
Sum of electronic and thermal Enthalpies= -2040.314322
Sum of electronic and thermal Free Energies= -2040.433970

$3t_1$+($3H_2O$)b

Zero-point correction= 0.792252 (Hartree/Particle)
Thermal correction to Energy= 0.839327
Thermal correction to Enthalpy= 0.840272
Thermal correction to Gibbs Free Energy= 0.714974
Sum of electronic and zero-point Energies= -2040.389038
Sum of electronic and thermal Energies= -2040.341963
Sum of electronic and thermal Enthalpies= -2040.341019
Sum of electronic and thermal Free Energies= -2040.466316

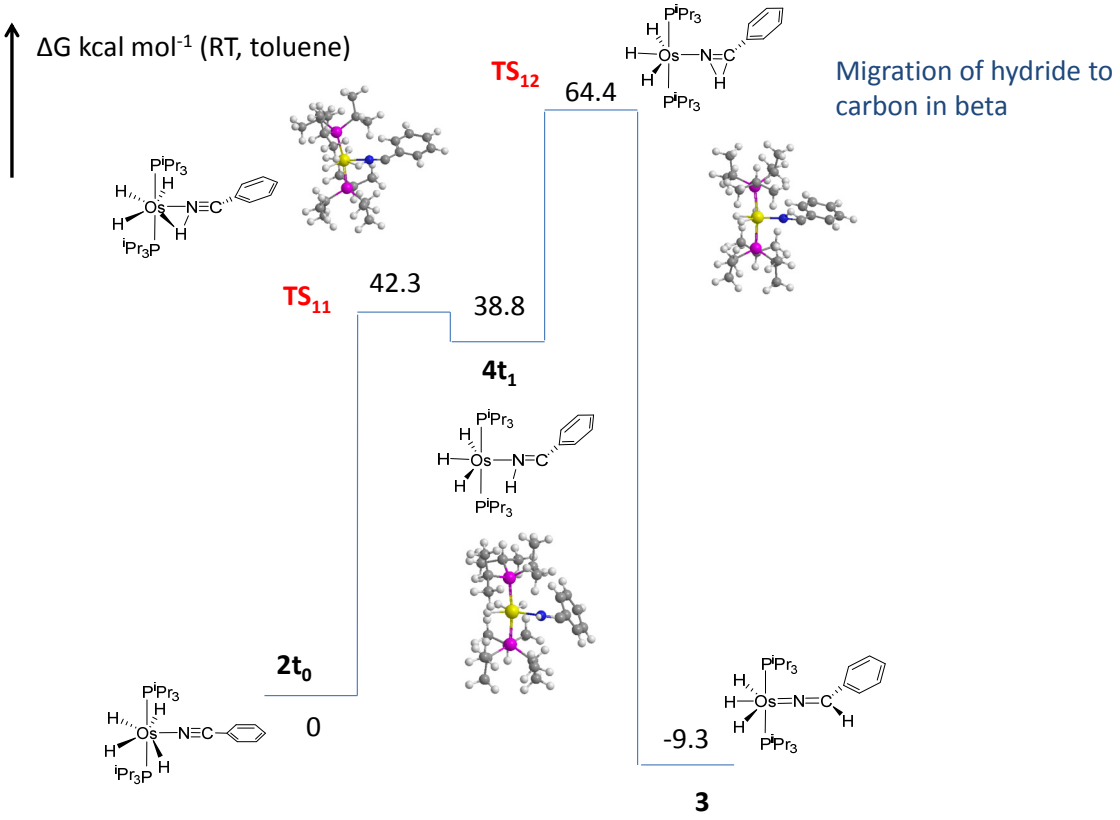

Figure S5. Computed energy profile for the migration of the hydride to the beta carbon atom of the nitrile.

TS11

Zero-point correction=	0.706851 (Hartree/Particle)
Thermal correction to Energy=	0.746039
Thermal correction to Enthalpy=	0.746983
Thermal correction to Gibbs Free Energy=	0.637587
Sum of electronic and zero-point Energies=	-1811.060515
Sum of electronic and thermal Energies=	-1811.021327
Sum of electronic and thermal Enthalpies=	-1811.020382
Sum of electronic and thermal Free Energies=	-1811.129779

$4t_1$

Zero-point correction=	0.711976 (Hartree/Particle)
Thermal correction to Energy=	0.751764
Thermal correction to Enthalpy=	0.752708
Thermal correction to Gibbs Free Energy=	0.641772
Sum of electronic and zero-point Energies=	-1811.065130
Sum of electronic and thermal Energies=	-1811.025343
Sum of electronic and thermal Enthalpies=	-1811.024399
Sum of electronic and thermal Free Energies=	-1811.135334

TS12

Zero-point correction=	0.706608 (Hartree/Particle)
Thermal correction to Energy=	0.746126
Thermal correction to Enthalpy=	0.747070
Thermal correction to Gibbs Free Energy=	0.637213
Sum of electronic and zero-point Energies=	-1811.025110
Sum of electronic and thermal Energies=	-1810.985592
Sum of electronic and thermal Enthalpies=	-1810.984648
Sum of electronic and thermal Free Energies=	-1811.094504

NMR and IR spectra of complexes 2, 3, 4, 5, 6, and 7.

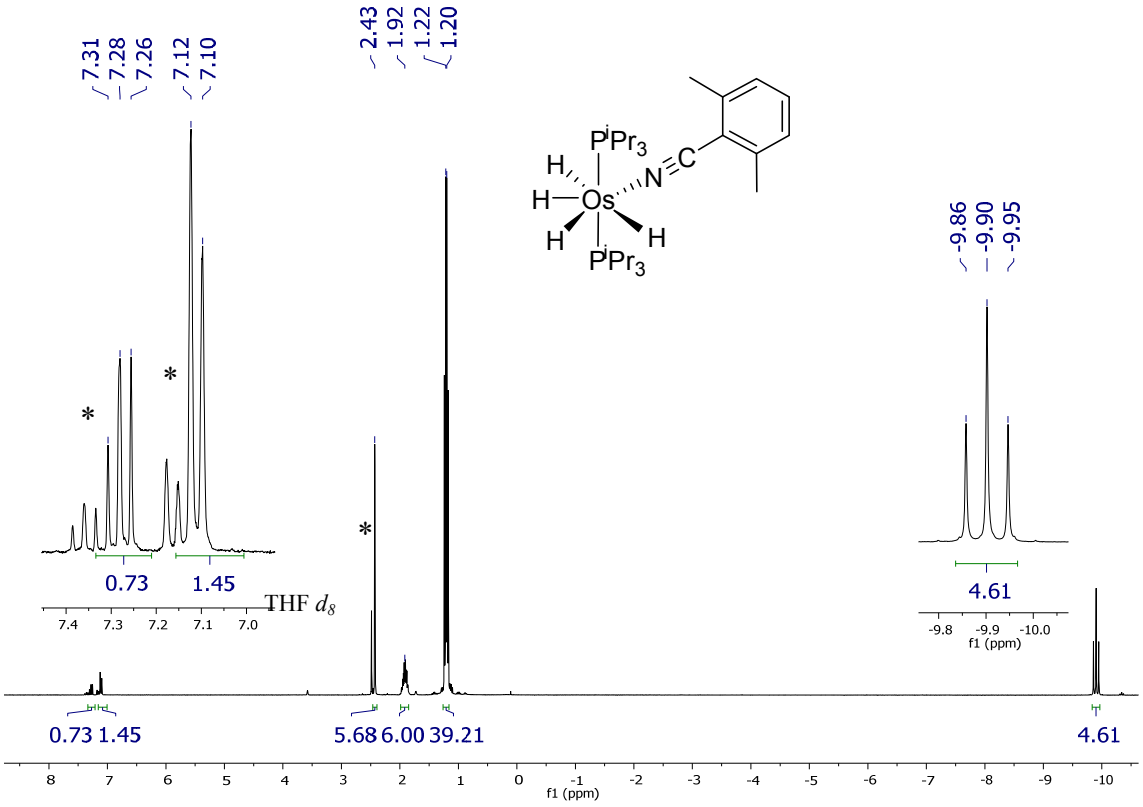

Figure S6. ^{1}H NMR (300.13 MHz, THF d_8, 298 K) spectrum for complex **2**. *Signals corresponding to free 2,6-dimethylbenzonitrile.

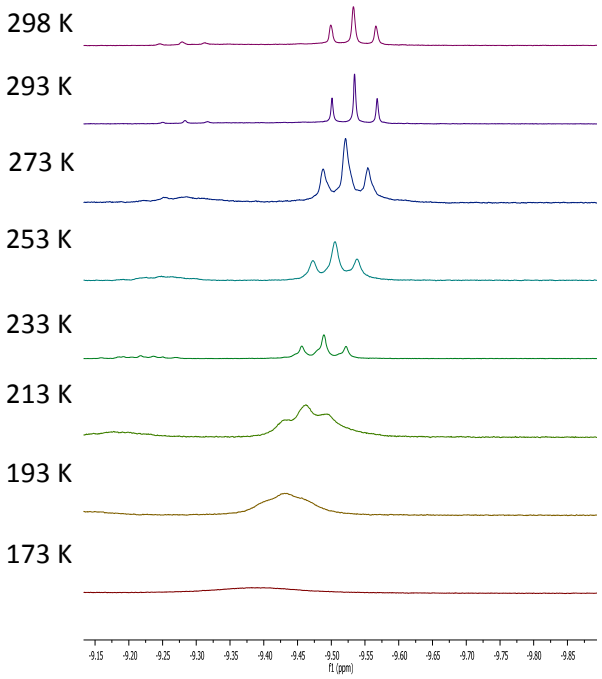

Figure S7. High-field region of the ^{1}H NMR (400.13 MHz, C_7D_8), spectrum of complex **2** between 298 and 173 K.

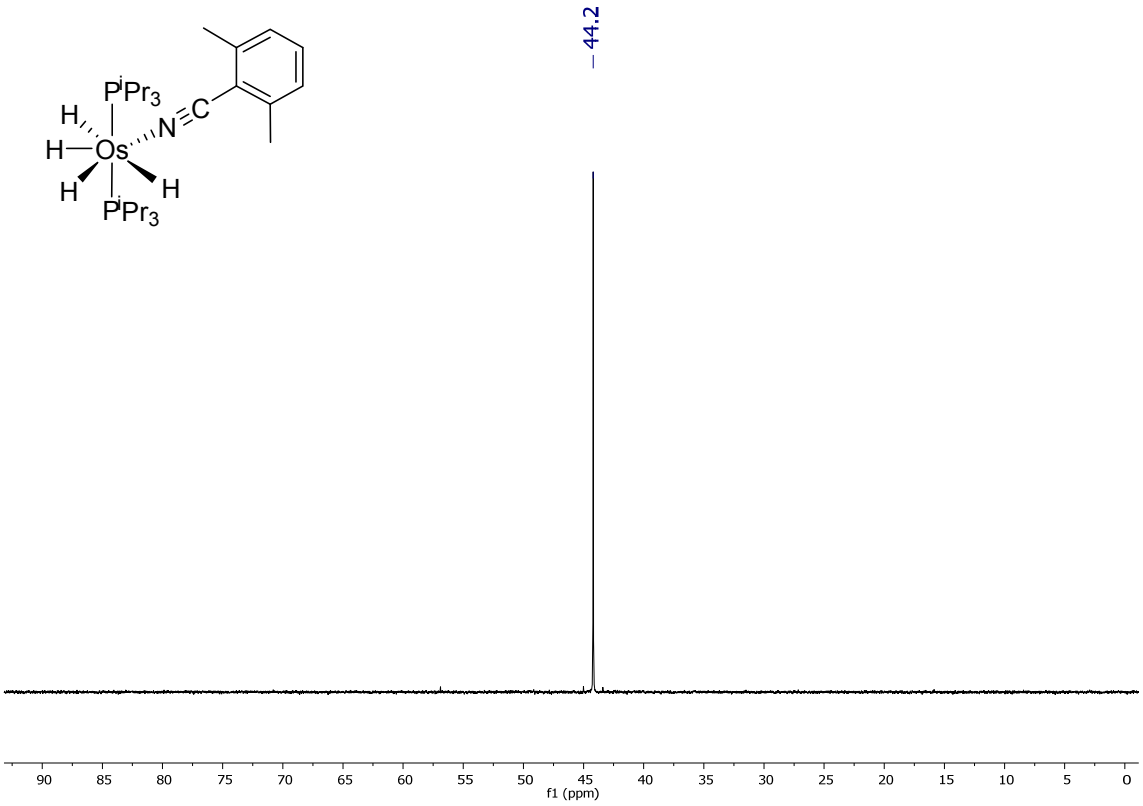

Figure S8. $^{31}P\{^1H\}$ NMR (121.49 MHz, THF d_8, 298 K) spectrum for complex **2**.

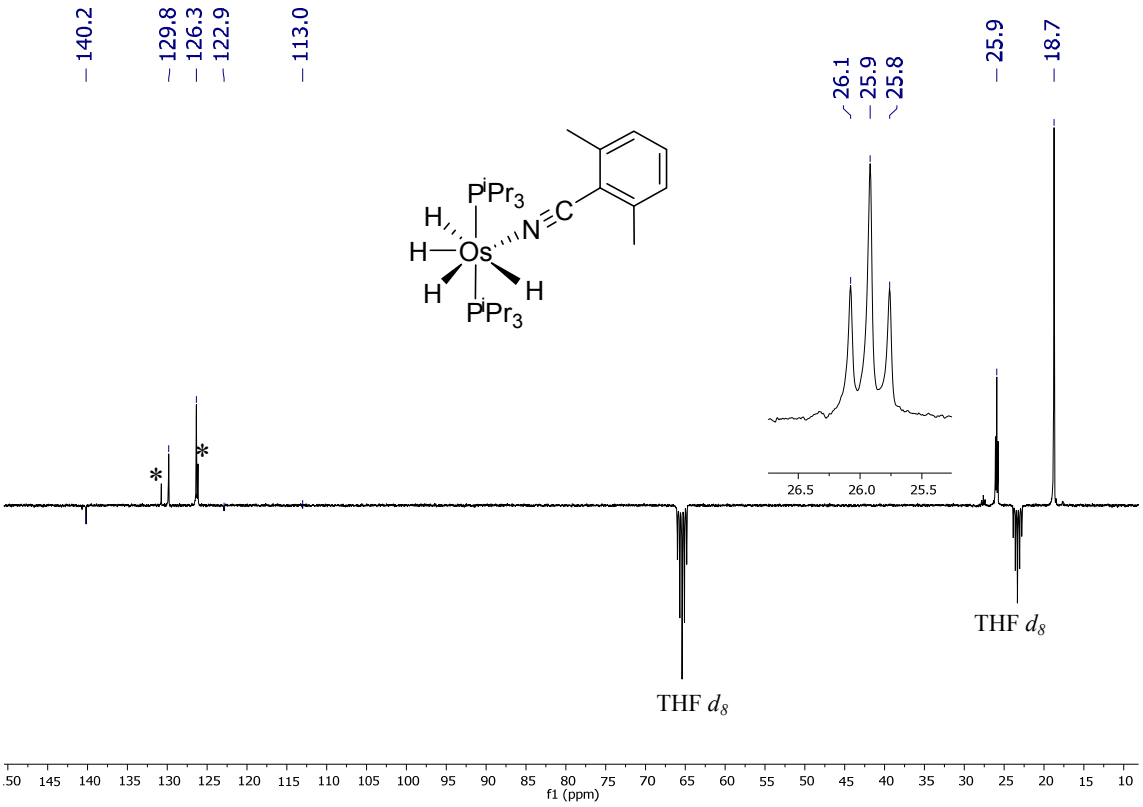

Figure S9. $^{13}C\{^1H\}$ APT NMR (75.48 MHz, THF d_8, 298 K) spectrum for complex **2**. *Signals corresponding to free 2,6-dimethylbenzonitrile.

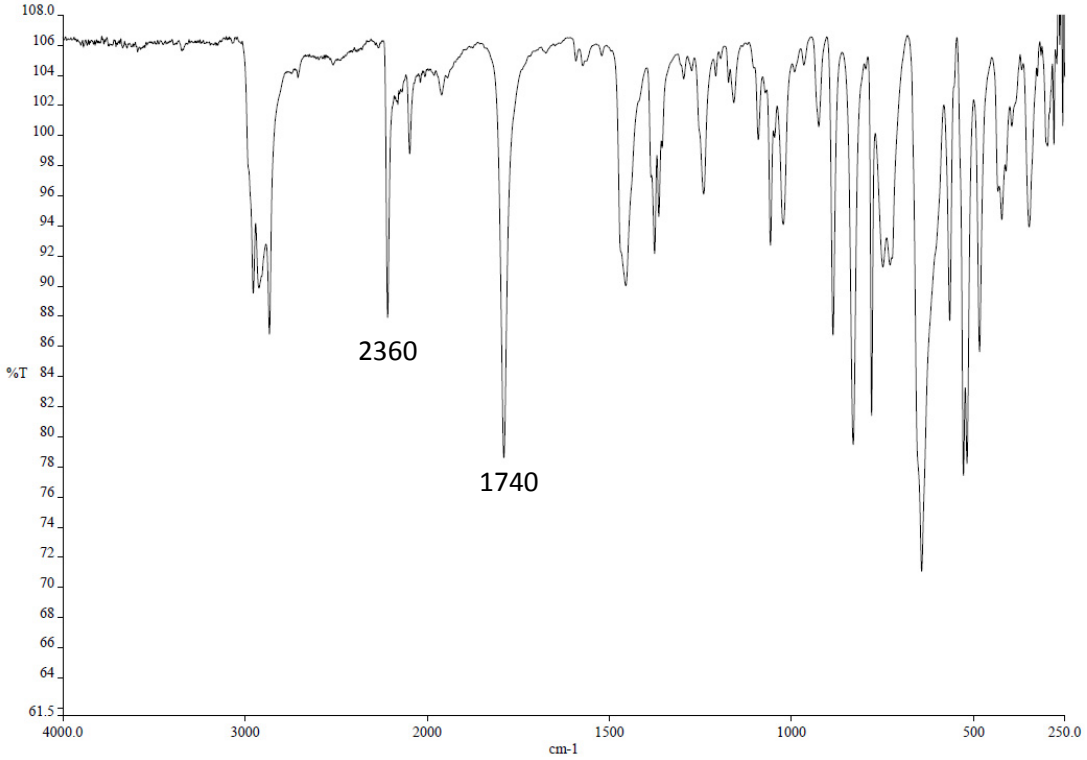

Figure S10. IR (ATR cm^{-1}) spectrum for complex **2**.

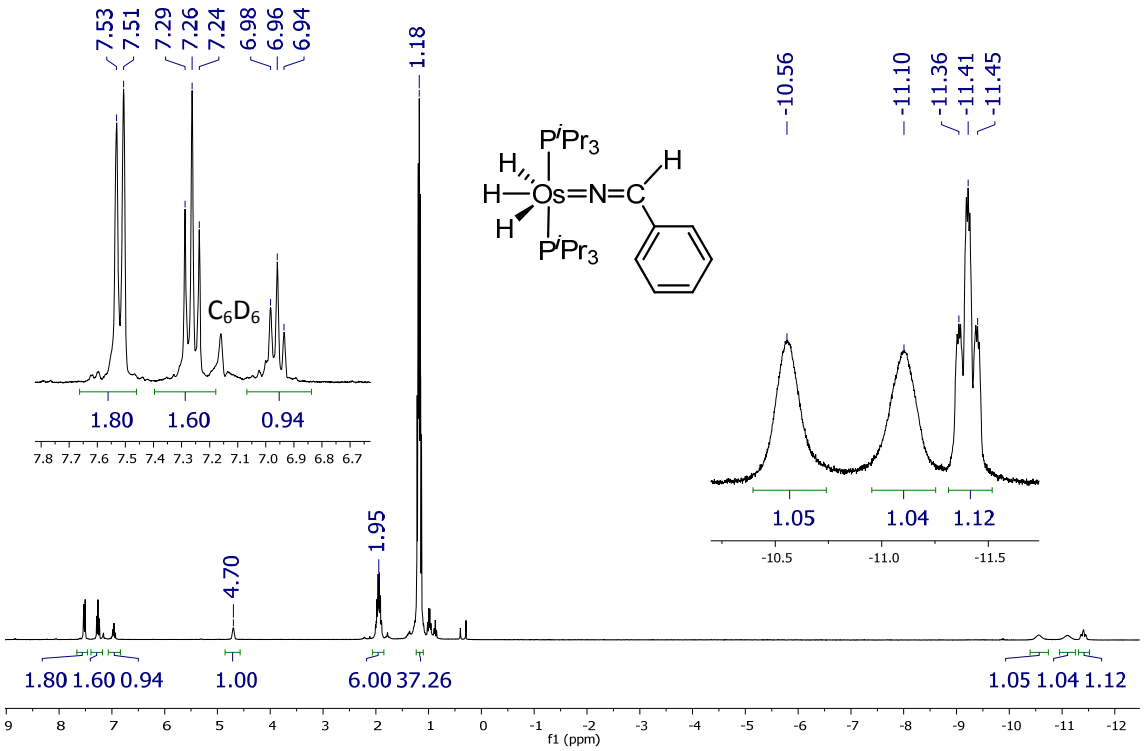

Figure S11. ^{1}H NMR (300.13 MHz, C_6D_6, 298 K) spectrum for complex **3**.

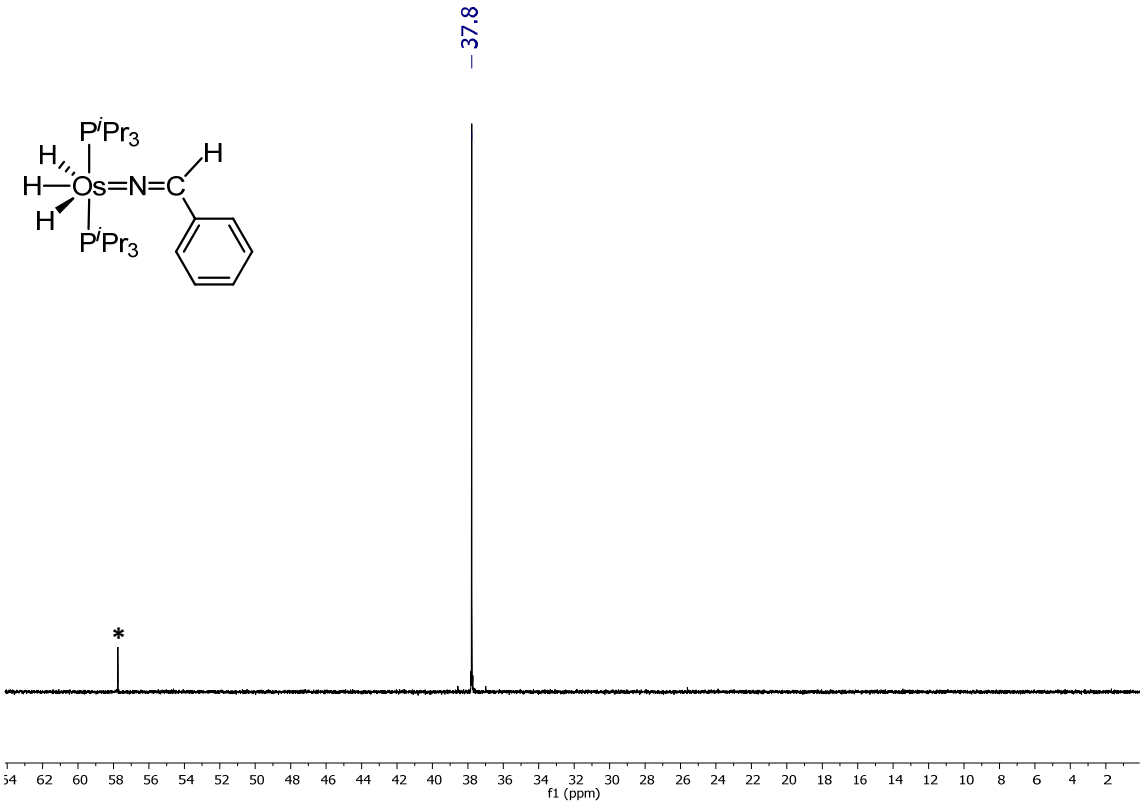

Figure S12. $^{31}P\{^1H\}$ NMR (121.49 MHz, C_6D_6, 298 K) spectrum for complex **3**. *Signal corresponding to complex **1**.

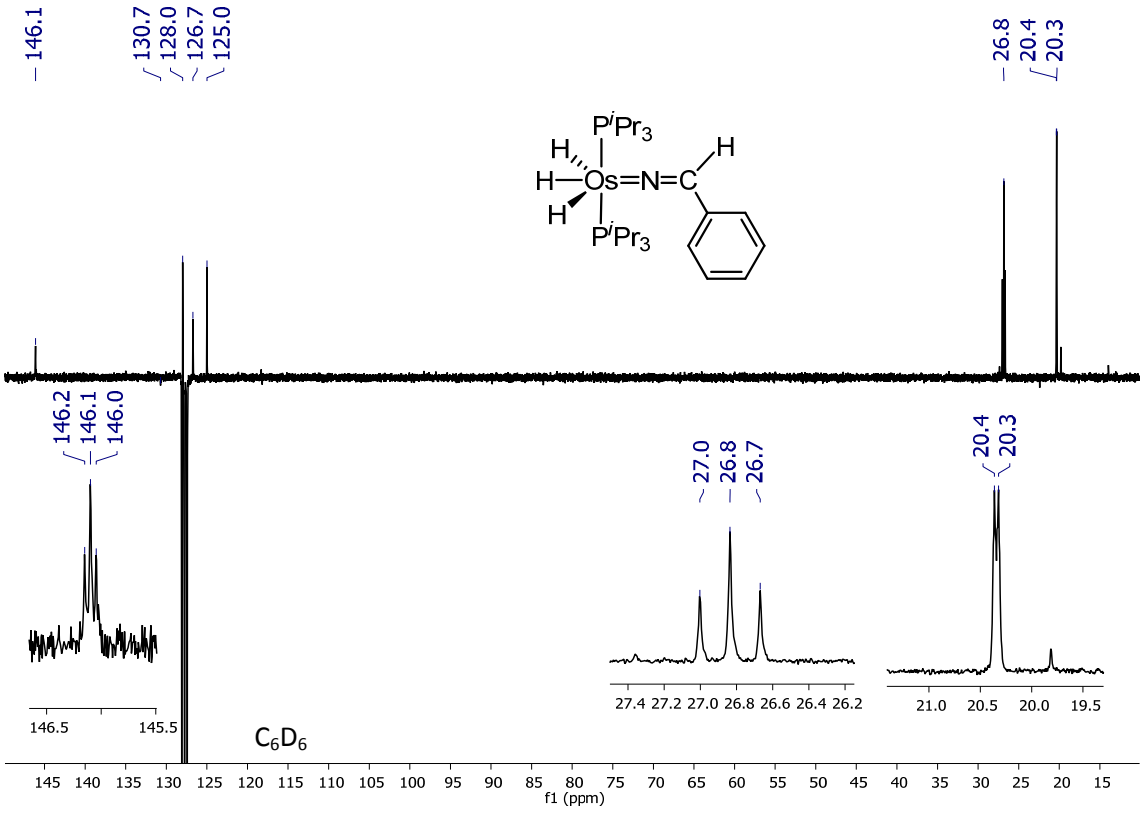

Figure S13. $^{13}C\{^1H\}$ APT NMR (75.48 MHz, C_6D_6, 298 K) spectrum for complex **3**.

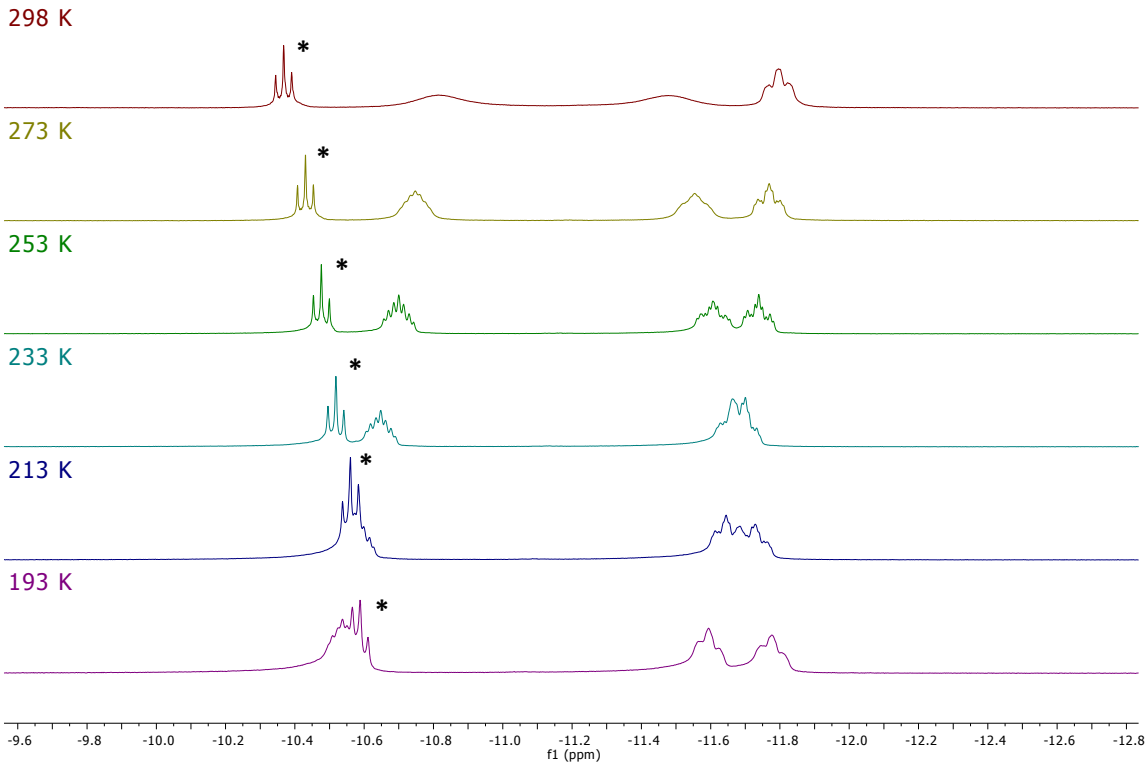

Figure S14. High-field region of the ^{1}H NMR (400.13 MHz, CD_2Cl_2) spectrum of complex **3** between 298 and 193 K. *Signal corresponding to complex **1**.

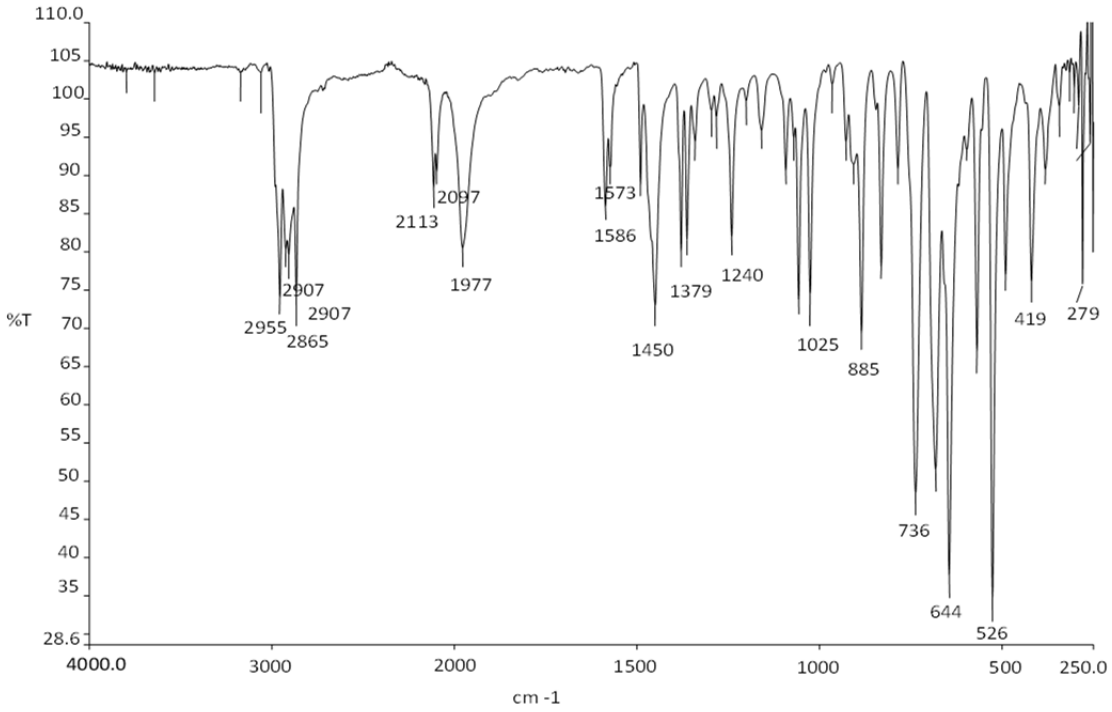

Figure S15. IR (ATR, cm^{-1}) spectrum for complex **3**.

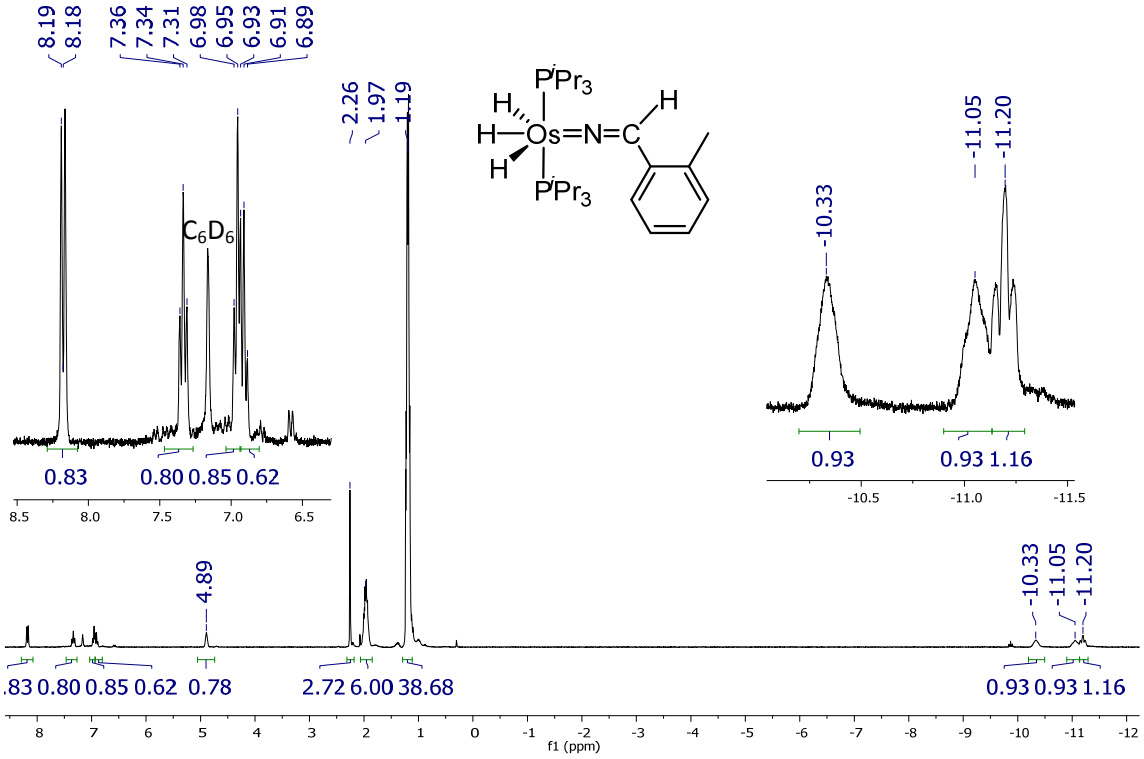

Figure S16. ^{1}H NMR (300.13 MHz, C_6D_6, 298 K) spectrum for complex **4**.

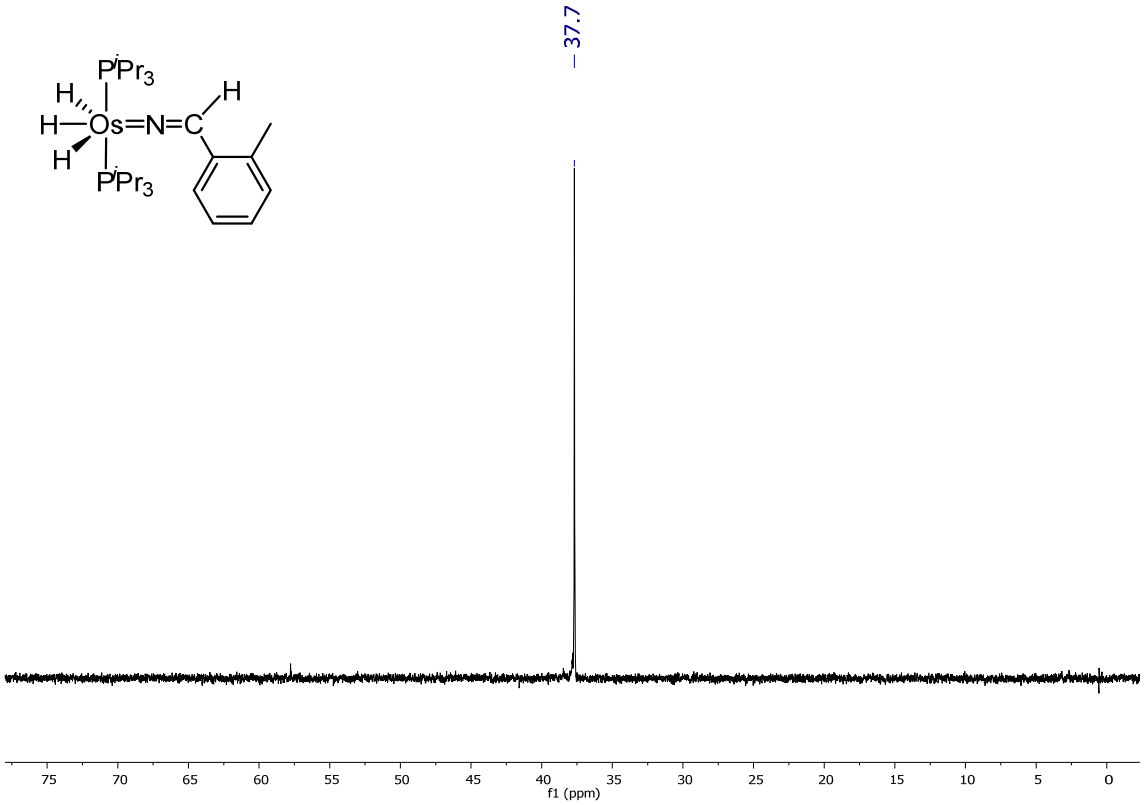

Figure S17. ^{31}P{^{1}H} NMR (121.49 MHz, C_6D_6, 298 K) spectrum for complex **4**.

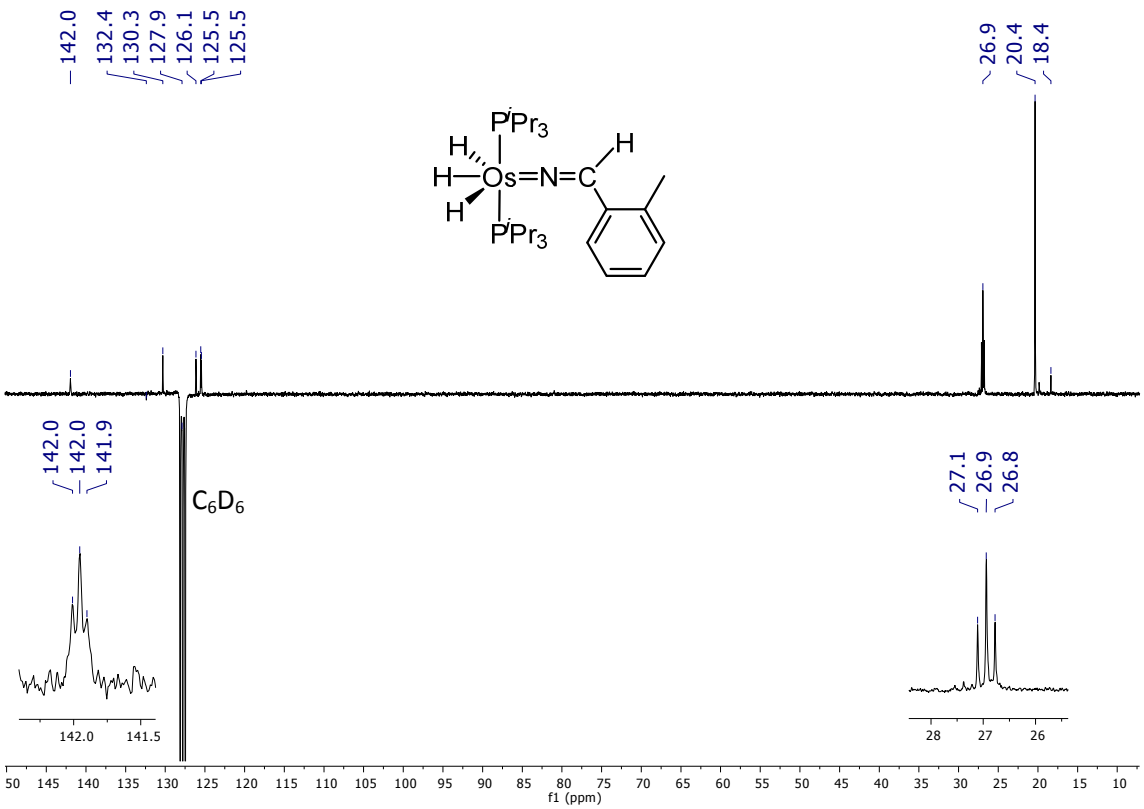

Figure S18. $^{13}C\{^1H\}$ APT NMR (75.48 MHz, C_6D_6, 298 K) spectrum for complex **4**.

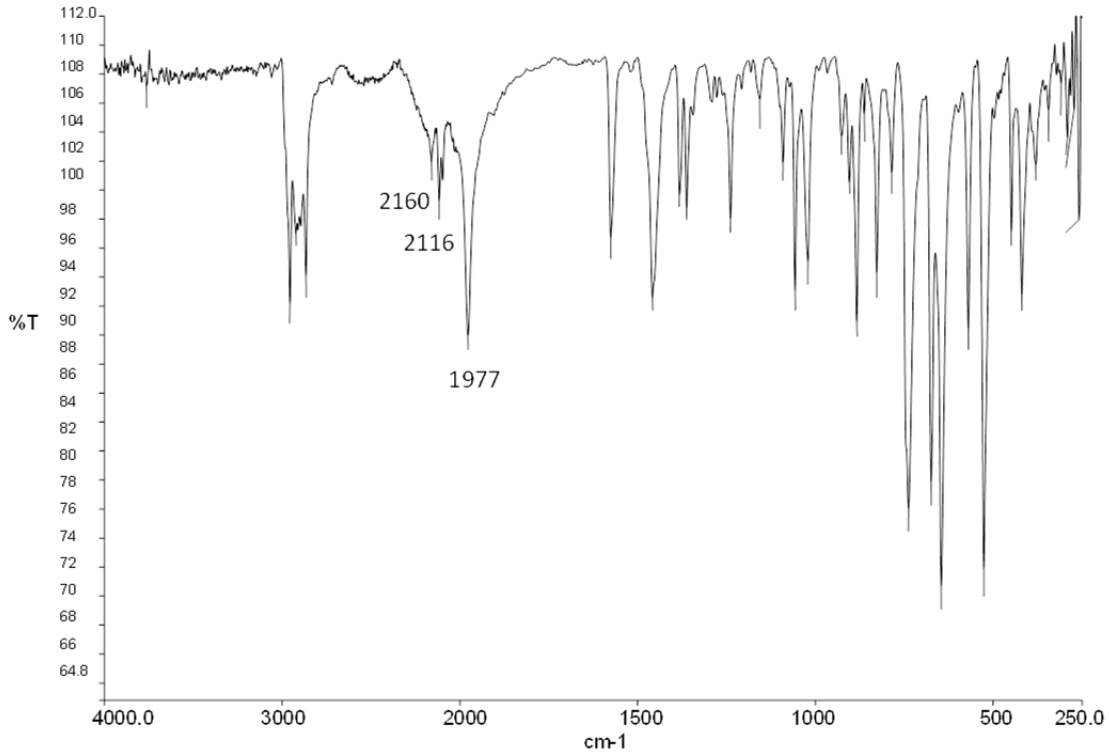

Figure S19. IR (ATR, cm^{-1}) spectrum for complex **4**.

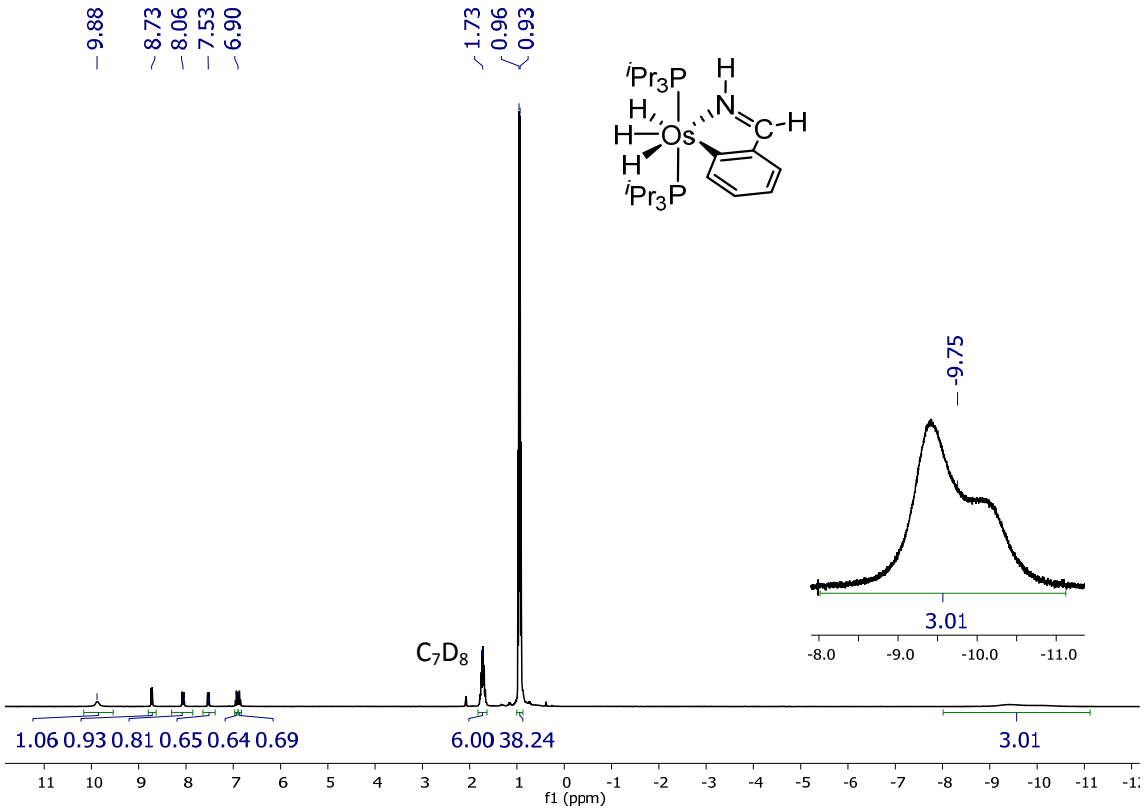

Figure S20. ^{1}H NMR (400.13 MHz, C_7D_8, 298 K) spectrum for complex **5**.

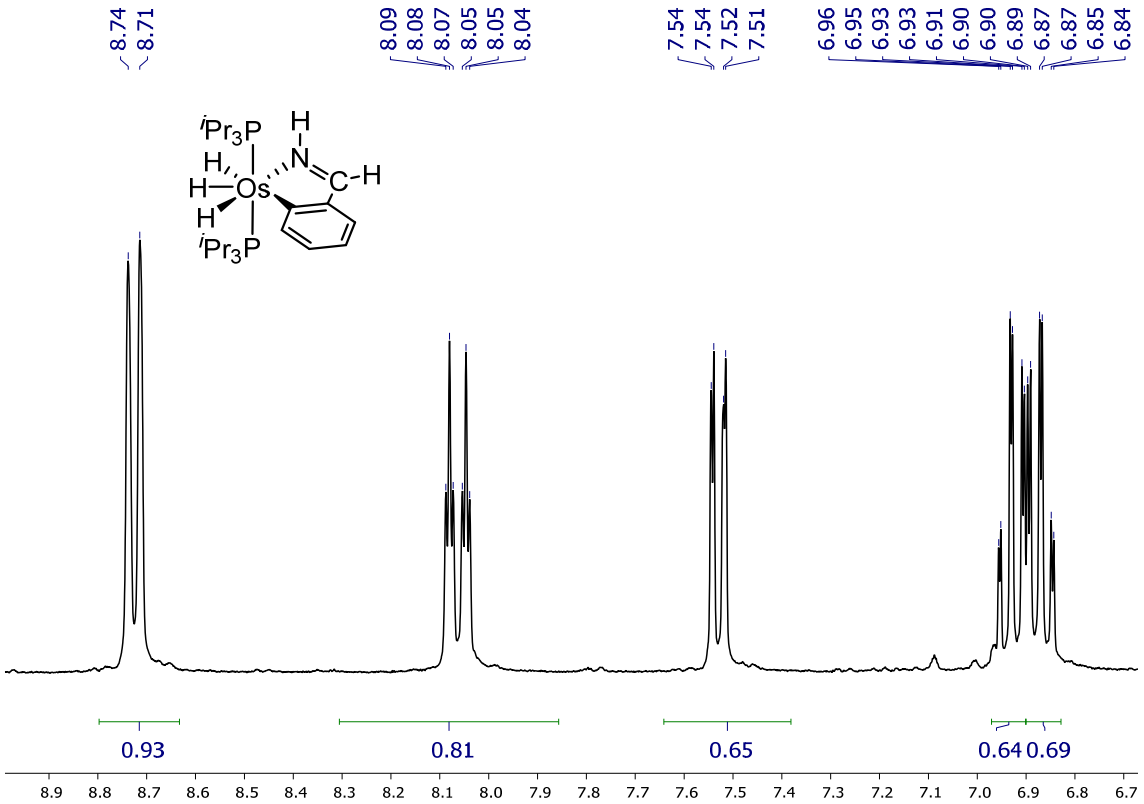

Figure S21. Low-field region of the ^{1}H NMR (400.13 MHz, C_7D_8, 298 K) spectrum of complex **5**.

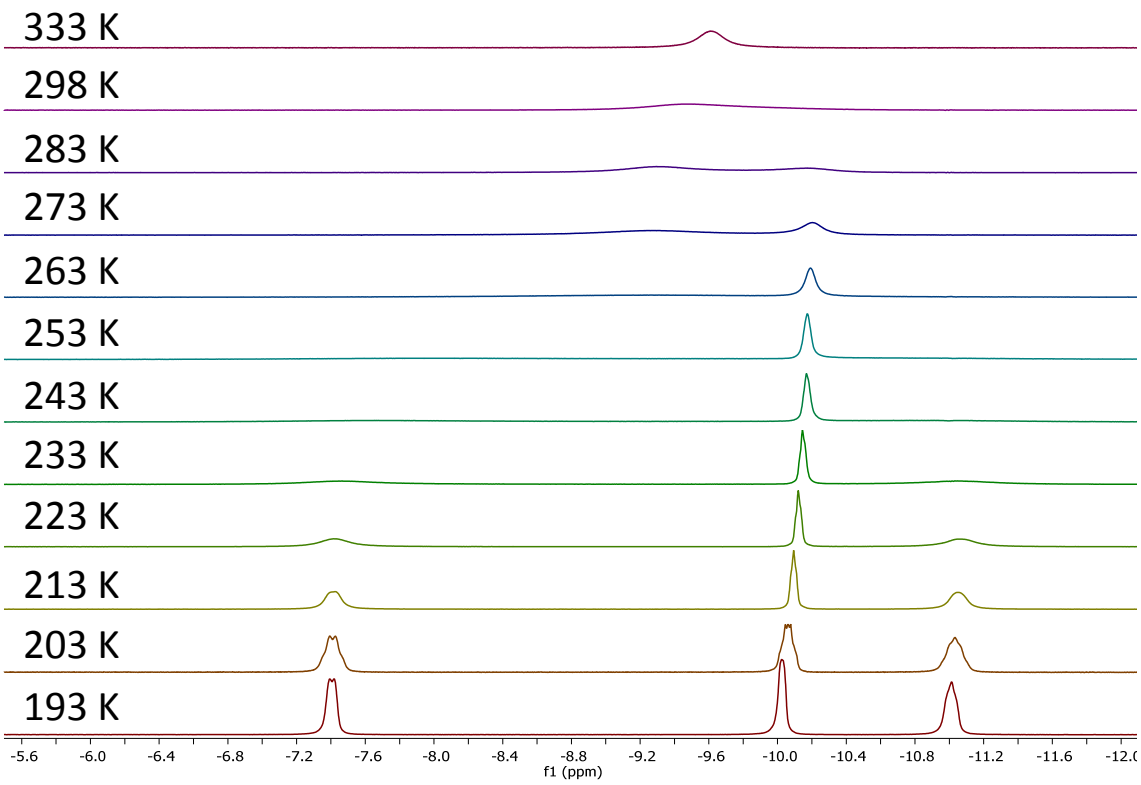

Figure S22. High-field region of the ^{1}H NMR (400.13 MHz, C_7D_8) spectrum of complex **5** between 333 and 193 K.

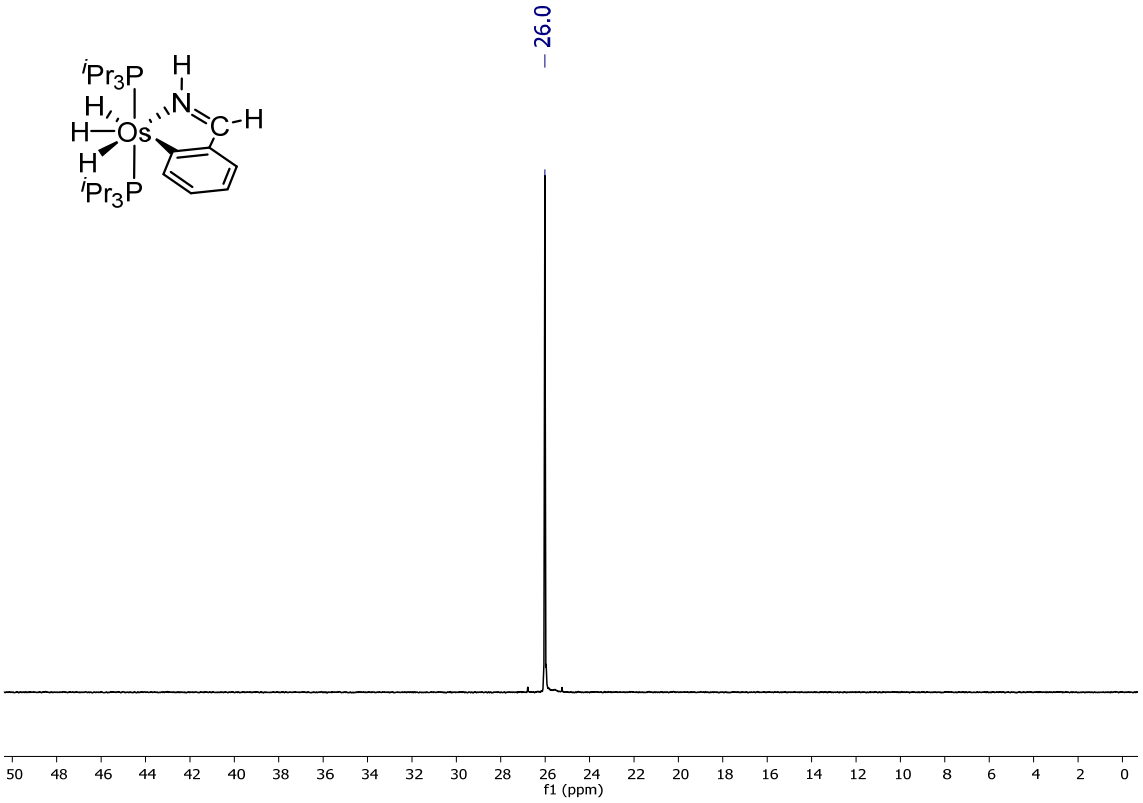

Figure S23. $^{31}P\{^{1}H\}$ NMR (121.49 MHz, C_7D_8, 298 K) spectrum for complex **5**.

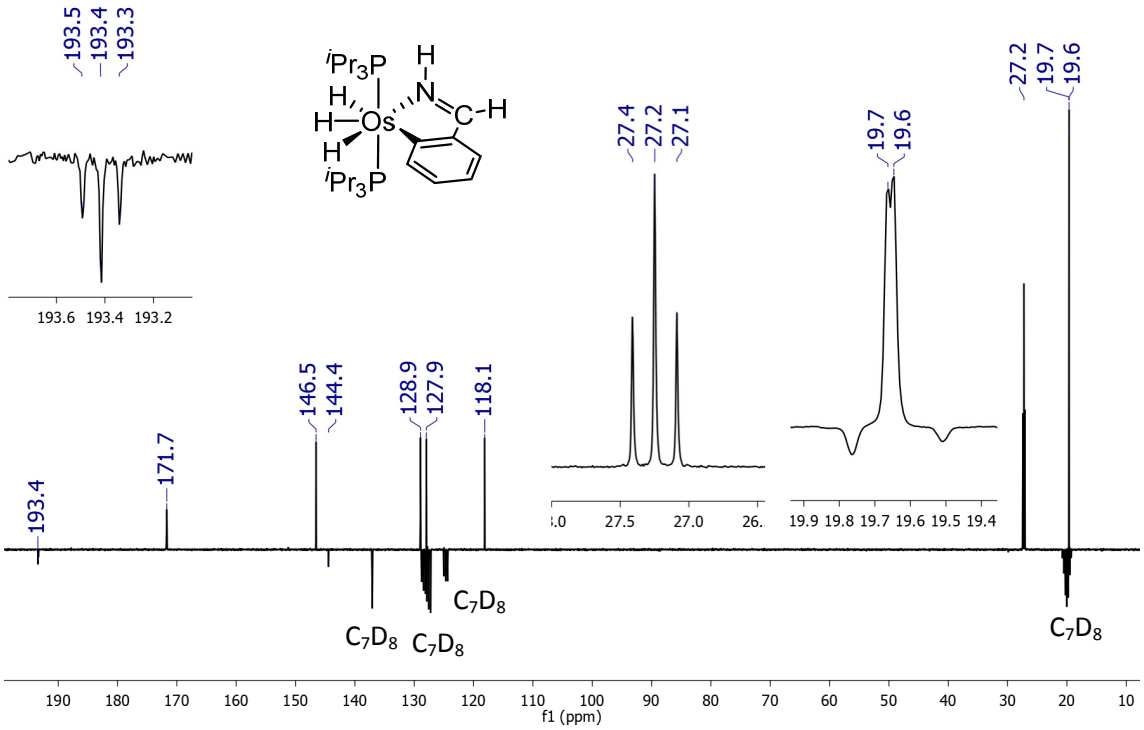

Figure S24. $^{13}C\{^{1}H\}$ APT NMR (75.48 MHz, C_7D_8, 298 K) spectrum for complex **5**.

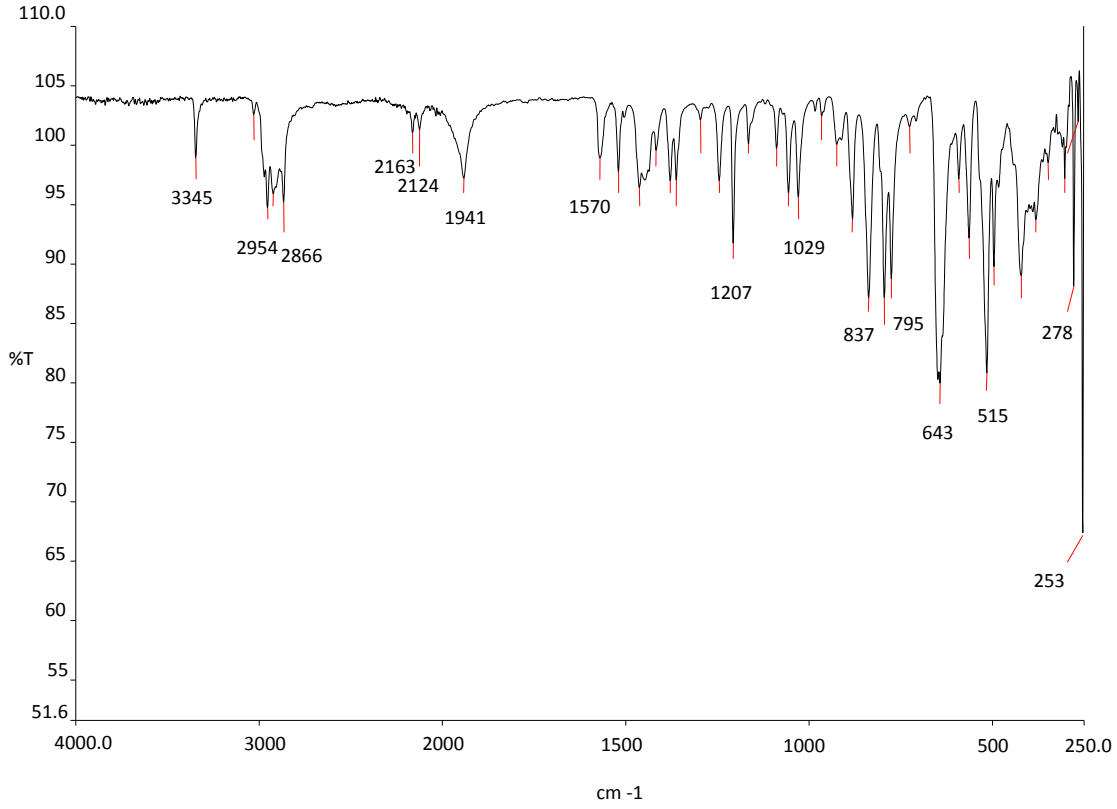

Figure S25. IR (ATR, cm^{-1}) spectrum for complex **5**.

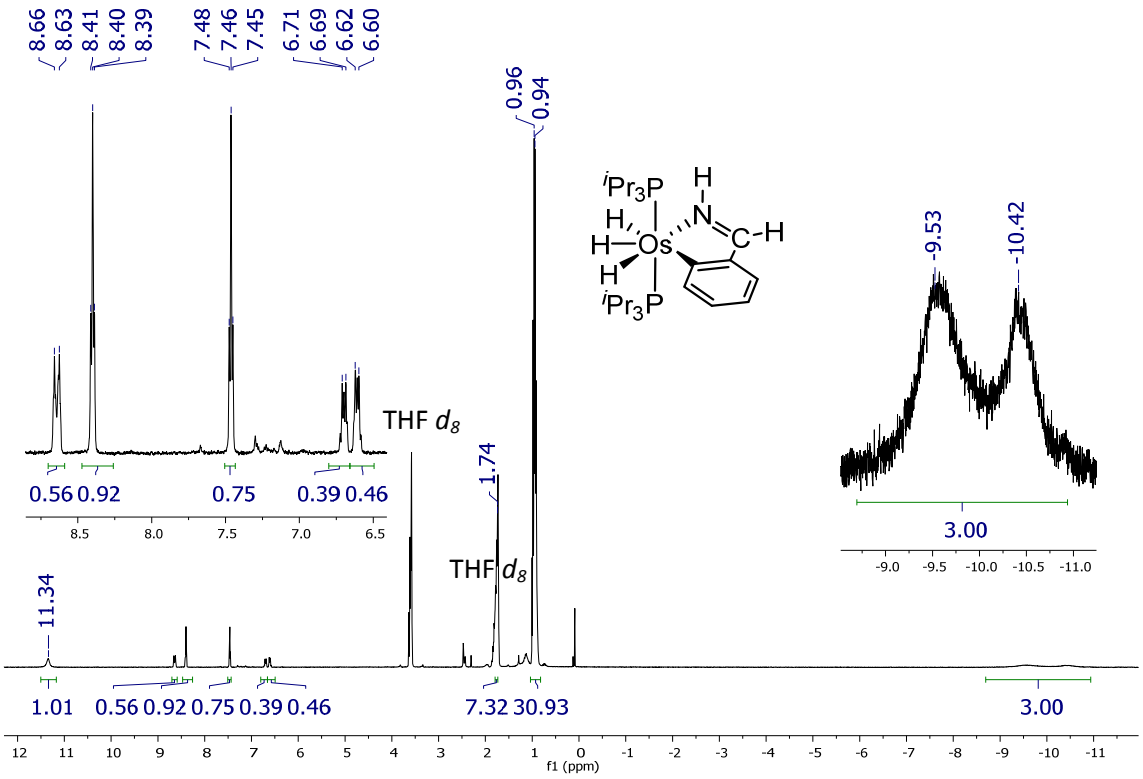

Figure S26. ^{1}H NMR (300.13 MHz, THF-d_8, 298 K) spectrum for complex **5**.

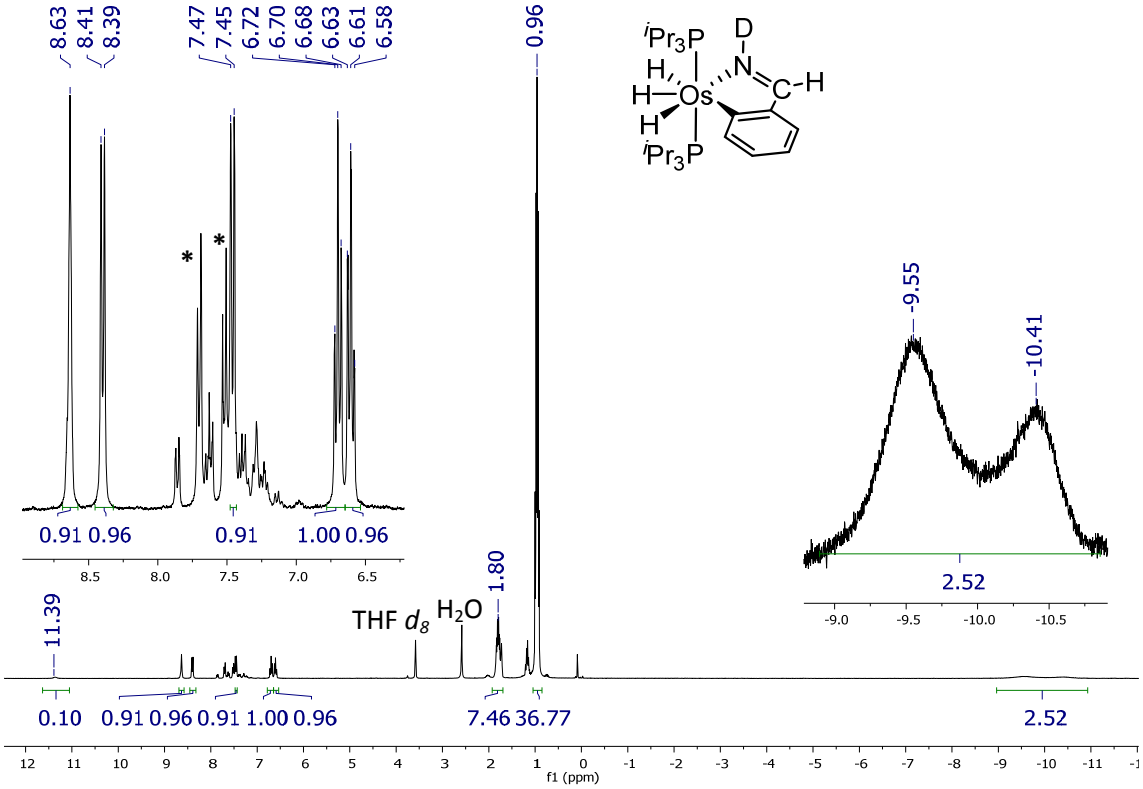

Figure S27. ^{1}H NMR (300.13 MHz, THF d_8, 298 K) spectrum for complex **5-*d***. *Signal corresponding to free benzonitrile.

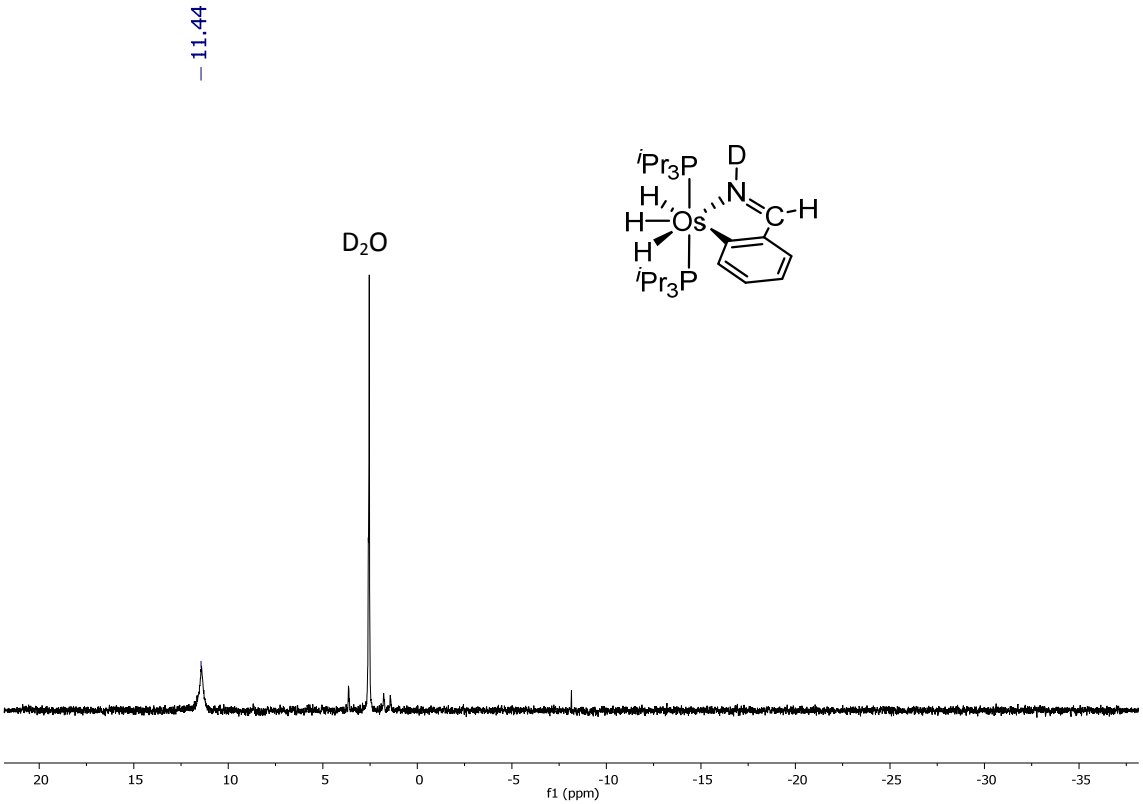

Figure S28. ^{2}H NMR (46.07 MHz, THF, 298 K) spectrum for complex **5-*d***.

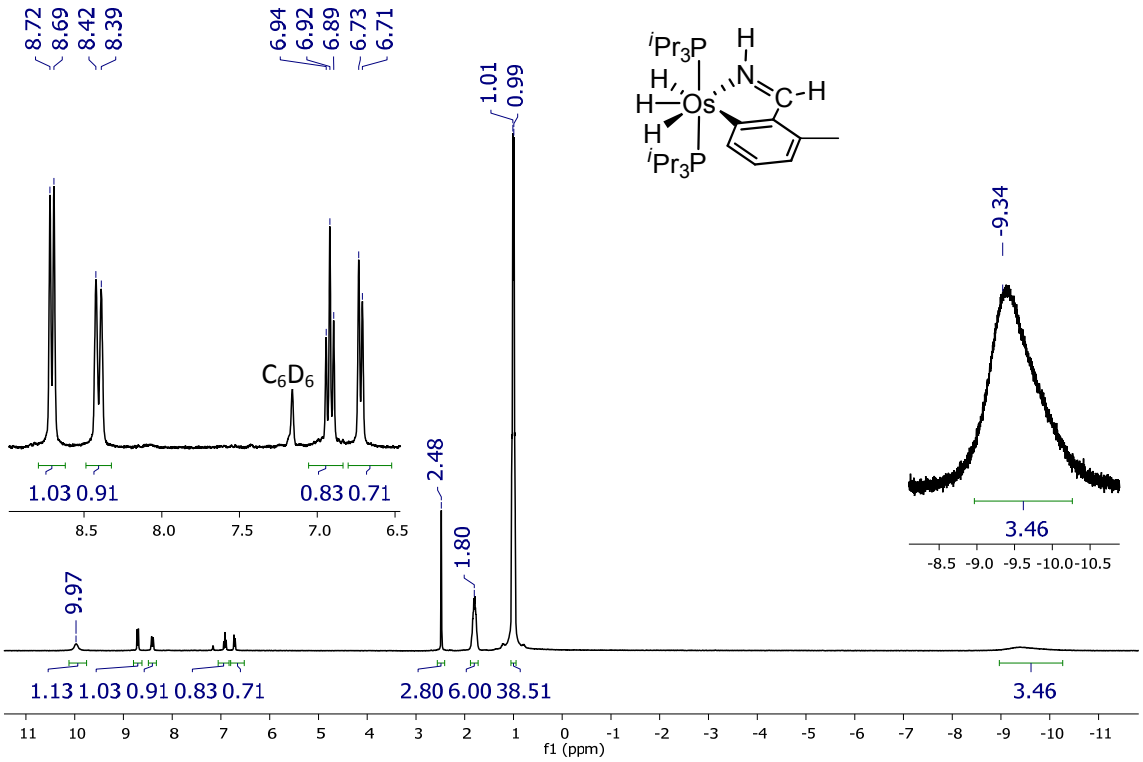

Figure S29. ^{1}H NMR (300.13 MHz, C_6D_6, 298 K) spectrum for complex **6**.

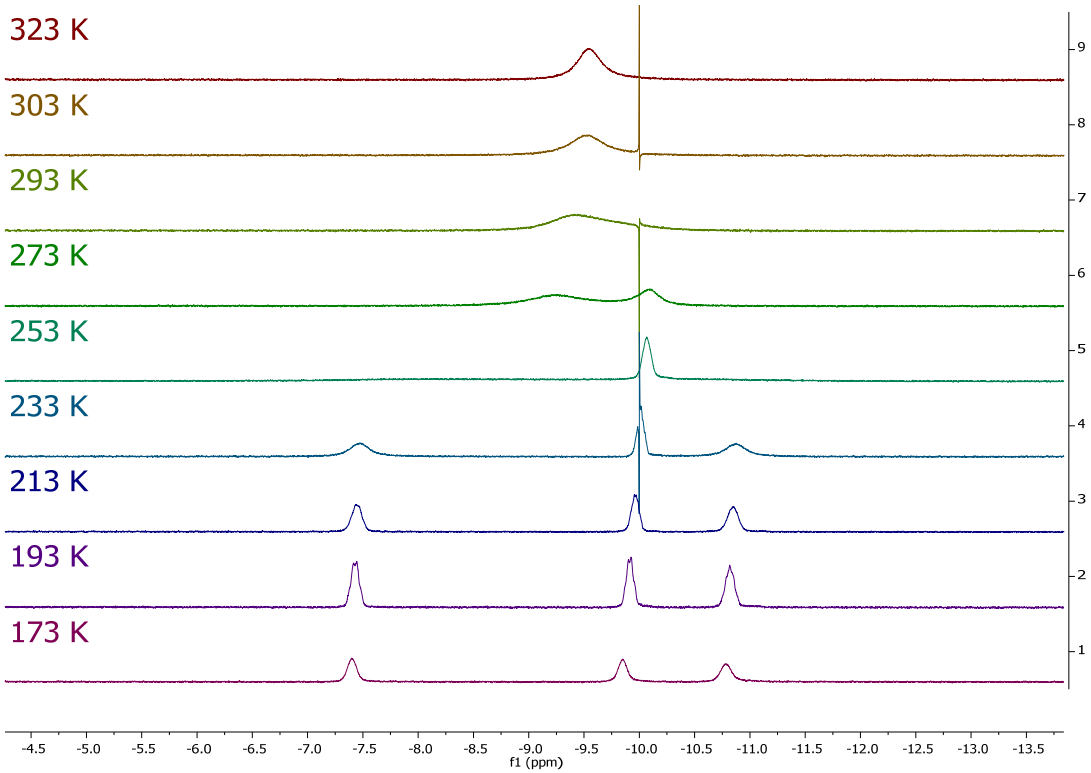

Figure S30. High-field region of the ^{1}H NMR (400.13 MHz, C_7D_8) spectrum of complex **6** between 323 and 173 K.

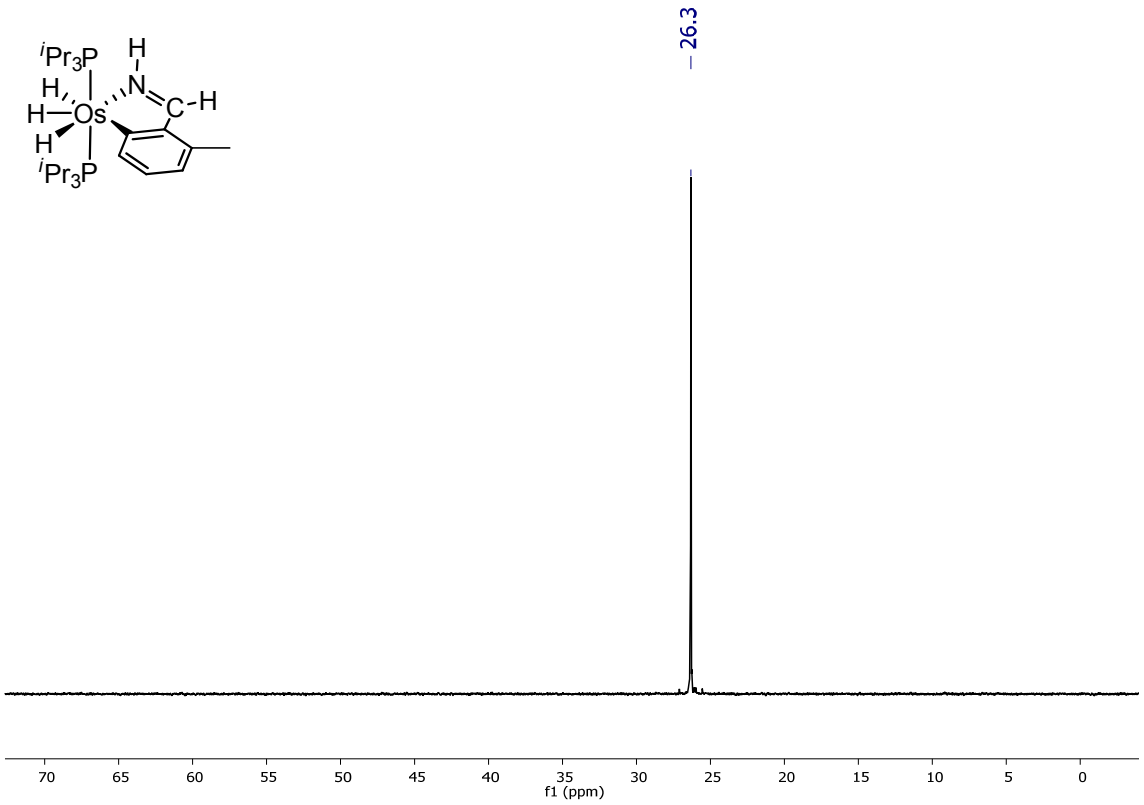

Figure S31. $^{31}P\{^{1}H\}$ NMR (121.49 MHz, C_6D_6, 298 K) spectrum for complex **6**.

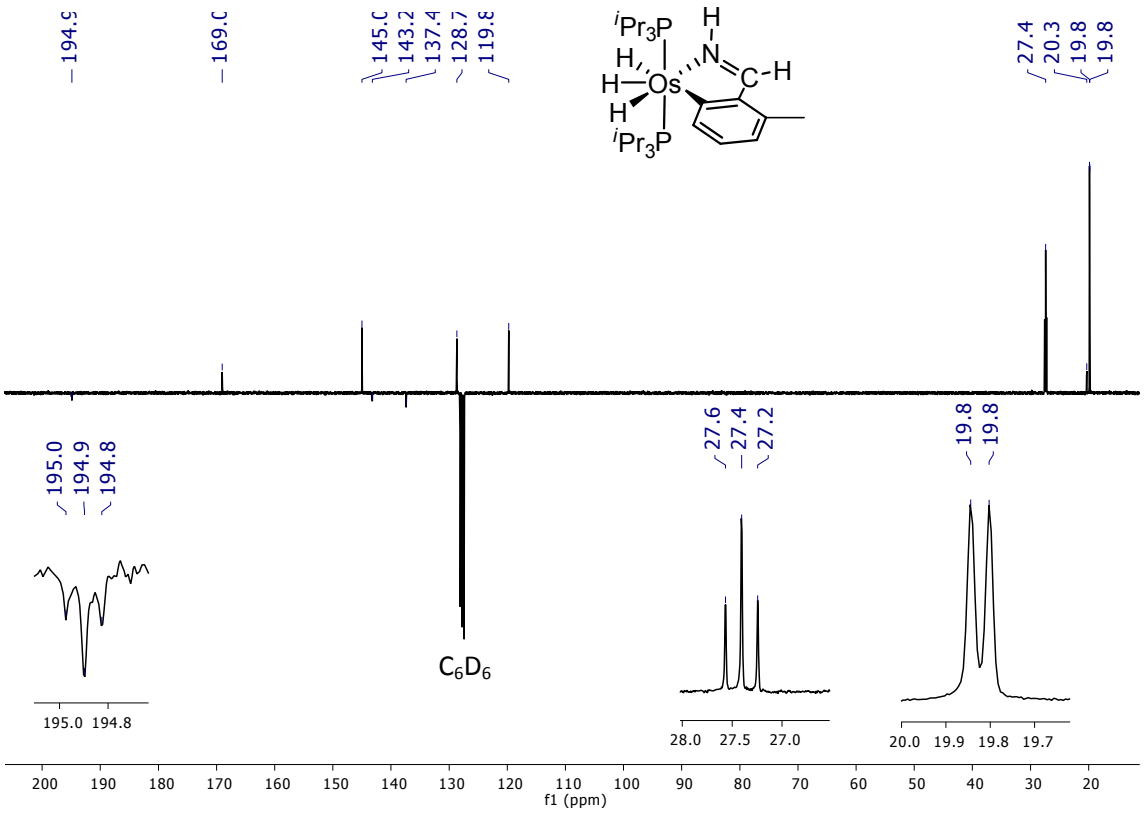

Figure S32. $^{13}C\{^{1}H\}$ APT NMR (75.48 MHz, C_6D_6, 298 K) spectrum for complex **6**.

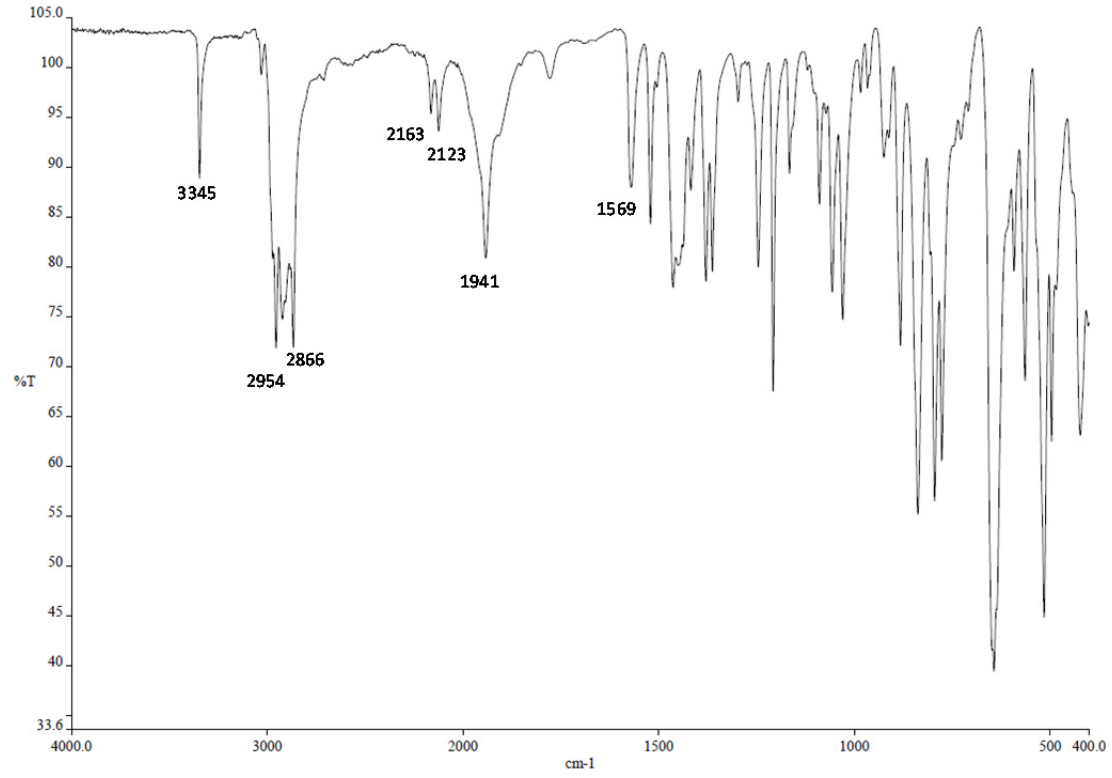

Figure S33. IR spectrum for complex **6**.

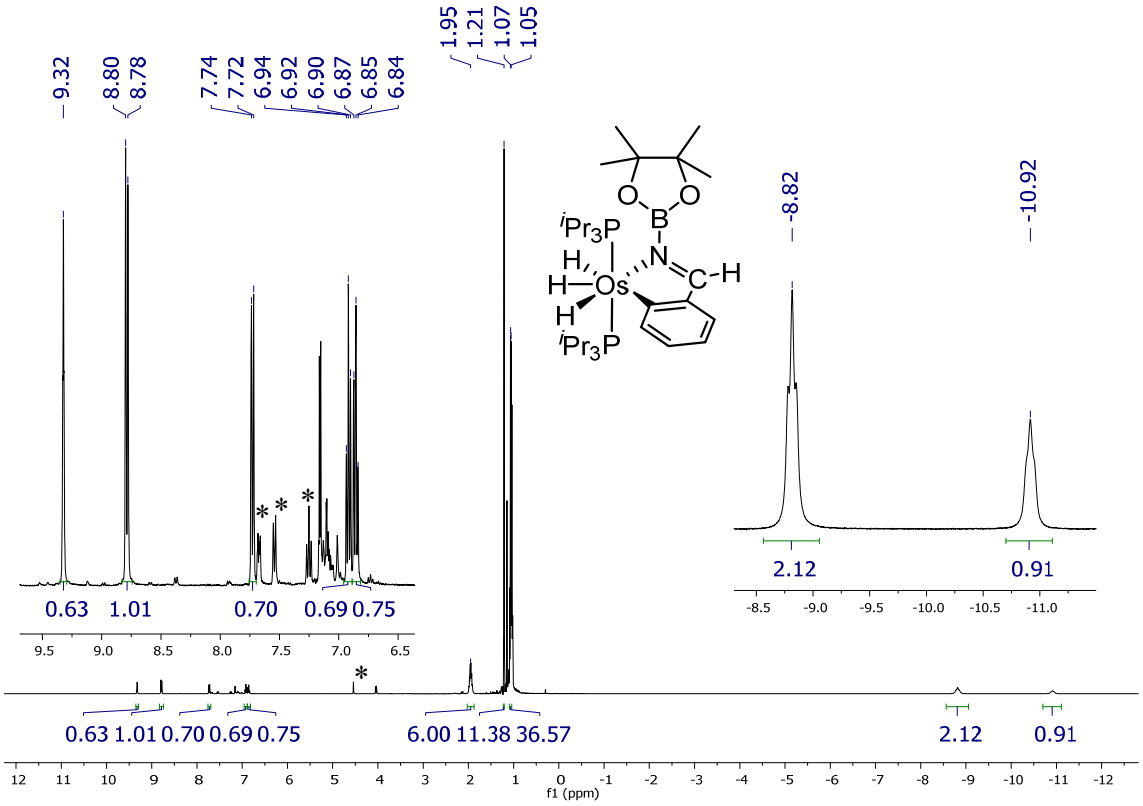

Figure S34. ^{1}H NMR (400.13 MHz, C_7D_8, 298 K) spectrum for complex **7**. *$PhCH_2N(Bpin)_2$.

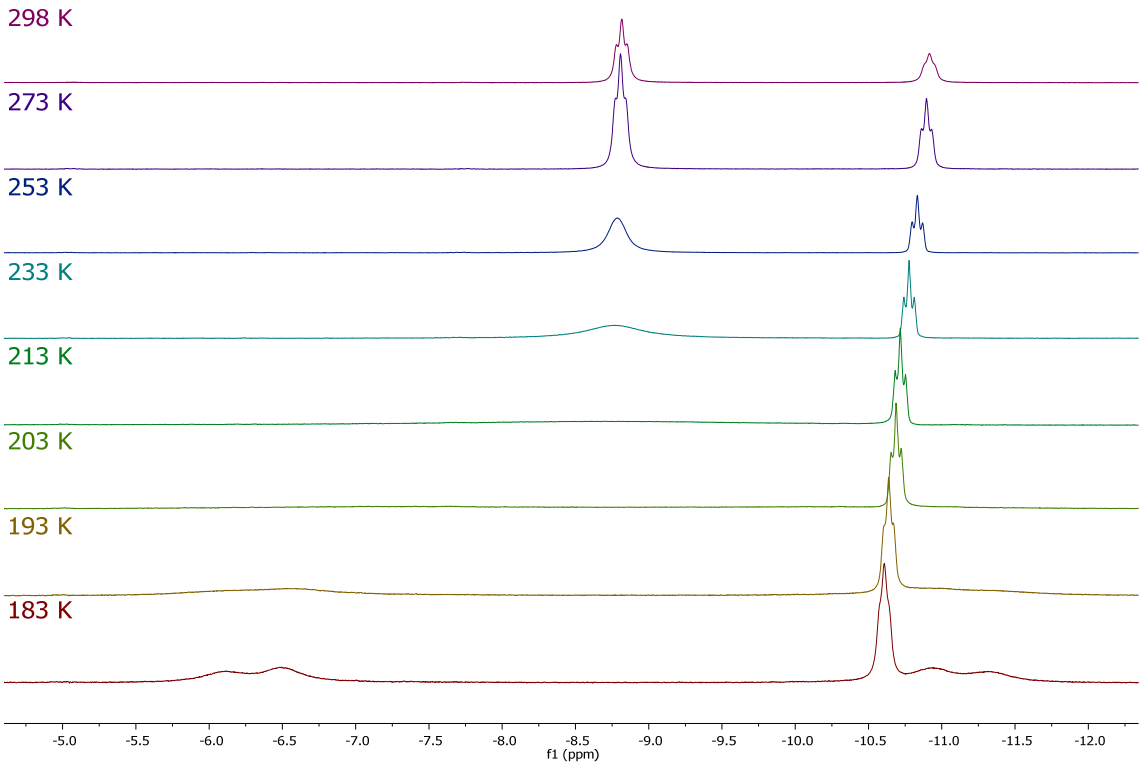

Figure S35. High-field region of the ^{1}H NMR (400.13 MHz, C_7D_8) spectrum of complex **7** between 298 and 183 K.

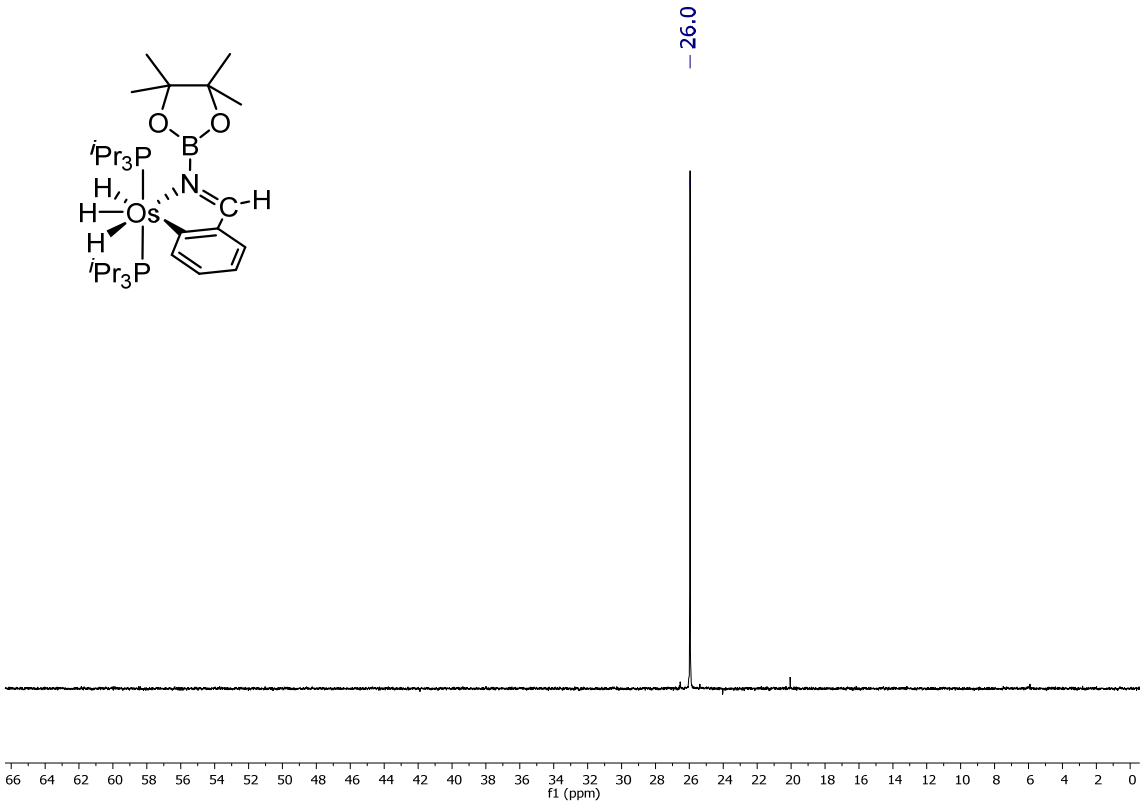

Figure S36. $^{31}P\{^{1}H\}$ NMR (121.49 MHz, C_7D_8, 298 K) spectrum for complex **7**.

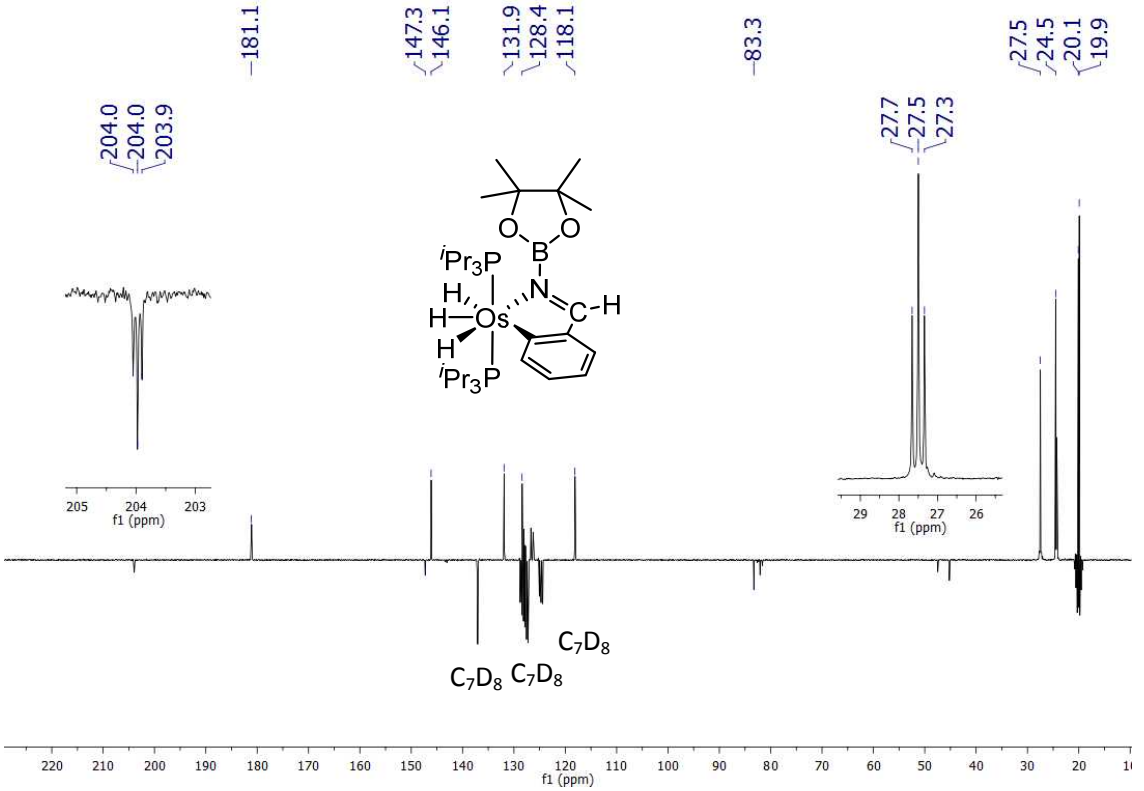

Figure S37. $^{13}C\{^{1}H\}$ APT NMR (75.48 MHz, C_7D_8, 298 K) spectrum for complex **7**.

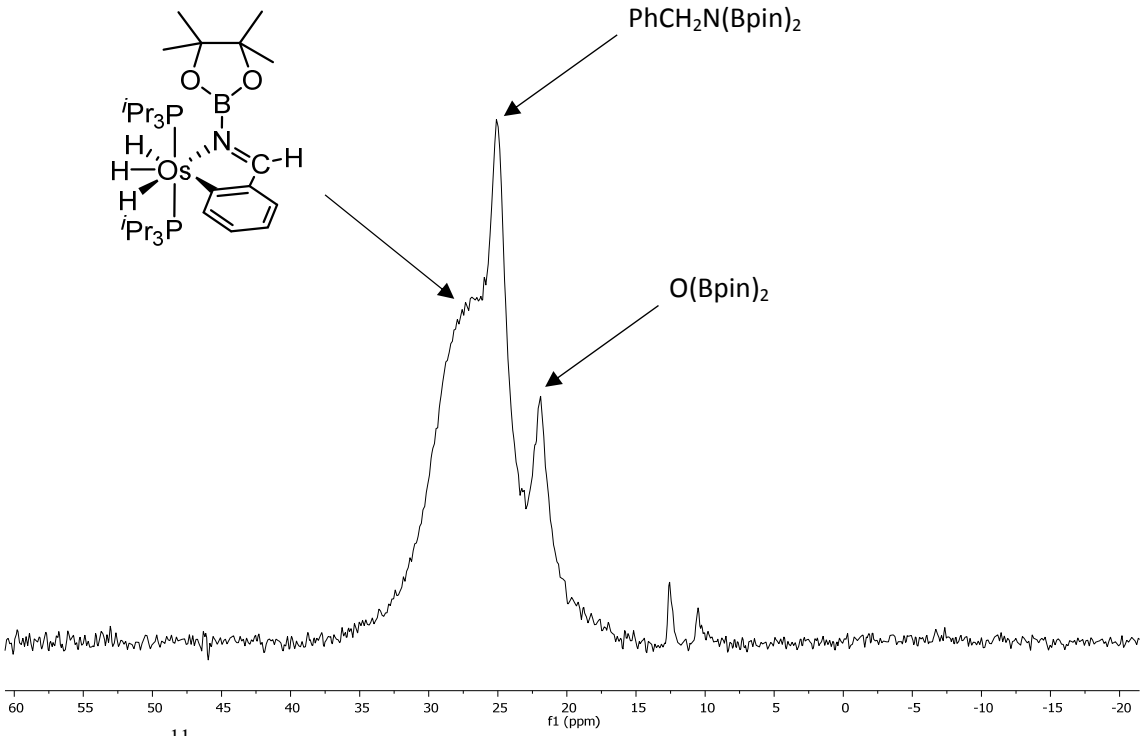

Figure S38. ^{11}B NMR (128.38 MHz, C_7D_8, 298 K) spectrum for complex **7**.

References

(1) Blessing, R. H. An Empirical Correction for Absorption Anisotropy. *Acta Crystallogr.* **1995**, *A51*, 33-38. *SADABS: Area-detector absorption correction*; Bruker-AXS, Madison, WI, 1996.

(2) SHELXL-2016/6. Sheldrick, G. M. A short history of SHELX. *Acta Cryst.* **2008**, *A64*, 112-122.

(3) Frisch, M. J.; Trucks, G. W.; Schlegel, H. B.; Scuseria, G. E.; Robb, M. A.; Cheeseman, J. R.; Scalmani, G.; Barone, V.; Mennucci, B.; Petersson, G. A.; Nakatsuji, H.; Caricato, M.; Li, X.; Hratchian, H. P.; Izmaylov, A. F.; Bloino, J.; Zheng, G.; Sonnenberg, J. L.; Hada, M.; Ehara, M.; Toyota, K.; Fukuda, R.; Hasegawa, J.; Ishida, M.; Nakajima, T.; Honda, Y.; Kitao, O.; Nakai, H.; Vreven, T.; Montgomery, J. A., Jr.; Peralta, J. E.; Ogliaro, F.; Bearpark, M.; Heyd, J. J.; Brothers, E.; Kudin, K. N.; Staroverov, V. N.; Kobayashi, R.; Normand, J.; Raghavachari, K.; Rendell, A.; Burant, J. C.; Iyengar, S. S.; Tomasi, J.; Cossi, M.; Rega, N.; Millam, J. M.; Klene, M.; Knox, J. E.; Cross, J. B.; Bakken, V.; Adamo, C.; Jaramillo, J.; Gomperts, R.; Stratmann, R. E.; Yazyev, O.; Austin, A. J.; Cammi, R.; Pomelli, C.; Ochterski, J. W.; Martin, R. L.; Morokuma, K.; Zakrzewski, V. G.; Voth, G. A.; Salvador, P.; Dannenberg, J. J.; Dapprich, S.; Daniels, A. D.; Farkas, Ö.; Foresman, J. B.; Ortiz, J. V.; Cioslowski, J.; Fox, D. J. *Gaussian 09, Revision D.01*; Gaussian, Inc., Wallingford CT, 2009.

(4) Becke, *A. D.* Density-functional exchange-energy approximation with correct asymptotic behavior. *Phys. Rev. A* **1988**, *38*, 3098-3100. (b) Perdew, J. P. Density-functional approximation for the correlation energy of the inhomogeneous electron gas *Phys. Rev. B* **1986**, *33*, 8822-8824.

(5) Weigend, F.; Ahlrichs, R. Balanced basis sets of split valence, triple zeta valence and quadruple zeta valence quality for H to Rn: Design and assessment of accuracy *Phys. Chem. Chem. Phys*. **2005**, *7*, 3297-3305.

(6) Grimme, S.; Antony, J.; Ehrlich, S.; Krieg, H. A consistent and accurate *ab initio* parametrization of density functional dispersion correction (DFT-D) for the 94 elements H-Pu. *J. Chem. Phys*. **2010**, *132*, 154104.

(7) Mitoraj, M. P.; Michalak, A.; Ziegler, T. A Combined Charge and Energy Decomposition Scheme for Bond Analysis. *J. Chem. Theory Comput*. **2009**, *5*, 962-975.

(8) von Hopffgarten, M.; Frenking, G. Energy decomposition analysis. *WIREs Comput. Mol. Sci*. **2012**, *2*, 43-62.

(9) Mitoraj, M. P.; Michalak, A. Natural orbitals for chemical valence as descriptors of chemical bonding in transition metal complexes. *J. Mol. Model*. **2007**, *13*, 347-355.

(10) See, for instance: (a) Mitoraj, M. P.; Michalak, A.; Ziegler, T. On the Nature of the Agostic Bond between Metal Centers and *β*-Hydrogen Atoms in Alkyl Complexes. An Analysis Based on the Extended Transition State Method and the Natural Orbitals for Chemical Valence Scheme (ETS-NOCV). *Organometallics* **2009**, *28*, 3727-3733. (b) Thi, A. N. N.; Frenking, G. *Chem. Eur. J.* **2012**, *18*, 12733. (c) Parafiniuk, M.; Mitoraj, M. P. Origin of Binding of Ammonia−Borane to Transition-Metal-Based Catalysts: An Insight from the Charge and Energy Decomposition Method ETS-NOCV. *Organometallics* **2013**, *32*, 4103-4113.

(11) ADF program: www.scm.com.

(12) Snijders, J. G.; Vernoojs, P.; Baerends, E. J. Roothaan-Hartree-Fock-Slater atomic wave functions: Single-zeta, double-zeta, and extended Slater-type basis sets for $_{87}$Fr-$_{103}$Lr. *At. Data. Nucl. Data Tables* **1981**, *26*, 483-509.

(13) Krijn, A.; Baerends, E. J.; *Fit Functions in the HFS-Method, Internal Report* (in Dutch), Vrije Universiteit Amsterdam, The Netherlands, 1984.

(14) (a) van Lenthe, E.; Baerends, E. J.; Snijders, J. G. Relativistic regular twocomponent Hamiltonians. *J. Chem. Phys.* **1993**, *99*, 4597–4610. (b) van Lenthe, E.; Baerends, E. J.; Snijders, J. G. Relativistic total energy using regular approximations. *J. Chem. Phys.* **1994**, *101*, 9783–9792. (c) van Lenthe, E.; Ehlers, A.; Baerends, E. J. Geometry optimizations in the zero order regular approximation for relativistic effects. *J. Chem. Phys.* **1999**, *110*, 8943–8953.